

Probing the inner structures of the observed Ξ_b and Ξ'_b resonances

Yu-Bin Zhang¹, Yi-Heng Wang¹, Hui-Hua Zhong² ^{*}, Li-Ye Xiao¹ [†]

¹)Institute of Theoretic al Physics, University of Science and Technology Beijing, Beijing 100083, China

²)College of Aeronautics Mechanical and Electrical Engineering, Jiangxi Flight University, Nanchang 330088, China

To shed light on the inner structure of the observed single-bottom strange baryons, in this work we systematically study the Okubo-Zweig-Iizuka allowed strong decay properties of $1P$ - and $2S$ -wave Ξ_b and Ξ'_b baryons within the $j-j$ coupling scheme in the framework of the quark pair creation model. For a comparison, we also give the predictions of the chiral quark model. The calculations indicate that: (i) The $1P$ -wave λ -mode Ξ_b states $\Xi_b|J^P = 1/2^-, 1\rangle_\lambda$ and $\Xi_b|J^P = 3/2^-, 1\rangle_\lambda$ are highly promising candidates for the observed state $\Xi_b(6087)$ and $\Xi_b(6095)/\Xi_b(6100)$, respectively. The $1P$ -wave ρ -mode Ξ_b states $\Xi_b|J^P = 3/2^-, 2\rangle_\rho$ and $\Xi_b|J^P = 5/2^-, 2\rangle_\rho$ are likely candidates for the state $\Xi_b(6227)$. Meanwhile, we cannot rule out the possibility that $\Xi_b(6227)$ could be a candidate of the $1P$ -wave λ -mode Ξ'_b state $\Xi'_b|J^P = 3/2^-, 2\rangle_\lambda$ or $\Xi'_b|J^P = 5/2^-, 2\rangle_\lambda$. (ii) For the other $1P$ -wave ρ -mode Ξ_b states and $1P$ -wave λ -mode Ξ'_b states, they may be moderate states with a width of several tens of MeV. Their main decay channels are $\Xi_b\pi$, $\Xi'_b\pi$, $\Xi_b^*\pi$ or $\Lambda_b\bar{K}$. The width of the $1P$ -wave ρ -mode Ξ'_b states are slightly broader, approximately several tens to over one hundred MeV, and the dominant decay channels are $\Xi'_b\pi$, $\Xi_b^*\pi$, $\Sigma_b K$ or $\Sigma_b^* K$. (iii) The $2S$ -wave λ -mode Ξ_b and Ξ'_b states are most likely to be relatively narrow state with a width of only a few to around ten MeV, and they mainly decay into $\Xi'_b\pi$ or $\Xi_b^*\pi$. In addition, the $2S$ -wave λ -mode Ξ'_b states may also mainly decay into the $1P$ -wave Ξ_b baryon via the pionic decay processes.

PACS numbers:

I. INTRODUCTION

Exploring internal structures and finding the missing resonance states is one of the important topics in hadronic physics, which will help us better understand strong interaction and the theoretical framework of nonperturbative quantum chromodynamics(QCD). Studies of hadrons containing a heavy quark play a special role since the heavy quark symmetry can be exploited.

There are a number of b baryon states that contain both beauty and strange quarks. The states form isospin doublets $\Xi_b^{(0,-)}$. In the quark model [1–3], three isospin doublets of ground states are expected. So far, five of these states have been observed in the experiment [4–7], only the Ξ_b^{*0} baryon remains unobserved. This is presumably because its mass lies below the threshold of $\Xi_b\pi^+$ [8] and makes it experimentally challenging to observed. Moreover, a great progress has been achieved on the observation of excited Ξ_b states. In 2018, the LHCb Collaboration firstly reported a resonance, $\Xi_b(6227)^-$, decaying into both $\Lambda_b^0 K^-$ and $\Xi_b^0 \pi^-$ [9]. Furthermore, the ratio of branching fractions were measured to be $B(\Xi_b(6227)^- \rightarrow \Lambda_b^0 K^-)/B(\Xi_b(6227)^- \rightarrow \Xi_b^0 \pi^-) \simeq 1.0 \pm 0.5$ [9], which provided a good reference for theoretical explanation. In 2021, the LHCb Collaboration confirmed this state again, and at the same time reported a new beauty-baryon resonance $\Xi_b(6227)^0$ decaying into $\Xi_b^-\pi^+$ [10]. The measured masses of the $\Xi_b(6227)^-$ and $\Xi_b(6227)^0$ states are consistent with them being isospin partners. Soon after, the CMS Collaboration clearly observed another narrow new resonance $\Xi_b(6100)^-$ near the $\Xi_b^-\pi^+\pi^-$ kinematic threshold [11]. And this new resonance was later confirmed by the LHCb

Collaboration in the $\Xi_b^{*0}(\Xi_b^-\pi^+)\pi^-$ mass distribution [12]. The $\Xi_b(6100)^-$ resonance and its decay sequence were consistent with the lightest orbitally excited Ξ_b^- baryon, with spin and parity quantum numbers $J^P = 3/2^-$ [11]. In 2022, two narrow resonant states, $\Xi_b(6327)^0$ and $\Xi_b(6333)^0$, were observed by the LHCb Collaboration again in the $\Lambda_b^0 K^- \pi^+$ mass spectrum, which properties were in good agreement with the expectations for a doublet of $1D$ Ξ_b^0 states [13]. Recently, the LHCb Collaboration announced again two new baryonic structures, $\Xi_b(6087)^0$ and $\Xi_b(6095)^0$, in the final state $\Xi_b^0 \pi^+ \pi^-$ [12]. And data indicated that the $\Xi_b(6087)^0$ baryon decayed mainly through the $\Xi_b^-\pi^+$ state and the $\Xi_b(6095)^0$ baryon mainly through the $\Xi_b^-\pi^+$ state [12]. Up to now there are twelve Ξ_b baryons observed experimentally according to the Particle Data Group [14] and we collect those states in Table I.

For constructing the highly excited bottom baryon spectroscopy, there exist many theoretical studies in the literature. Before the experiment, various theoretical models and calculations predicted the masses and decay properties of excited $\Xi_b^{(*)}$ baryons [15–22, 22–36], which established a valuable theoretical framework for experimental observation [11, 13]. After the experiment, a great deal of theoretical work was also stimulated to decode the inner structures of those newly observed states. For the heaviest observed excited states $\Xi_b(6327)^0$ and $\Xi_b(6333)^0$, the most popular explanation is interpreting them into $1D$ -wave Ξ_b resonances with spin-parity $J^P = 3/2^+$ and $5/2^+$ [37–42], respectively. Meanwhile, there are other interpretations, such as $1P$ - wave Ξ'_b states with spin-parity $J^P = 1/2^-$ [43, 44], $3/2^-$ [43–45] or $5/2^-$ [45]. For the first observed excited state $\Xi_b(6227)$, the theory explains it as $1P$ -wave Ξ'_b states [42, 46] with spin-parity $J^P = 1/2^-$ [47], $J^P = 3/2^-$ [36, 43, 45, 48–50], or $J^P = 5/2^-$ [36, 38, 39, 44, 49, 51]. Interpreted $\Xi_b(6227)$ as $2S$ -wave Ξ_b state [42] with spin-parity $J^P = 1/2^+$ [37, 43] is also allowed in theory. Besides the above conventional explanations, there exist some exotic explanations for the $\Xi_b(6227)$,

^{*}E-mail: zhonghuihua@foxmail.com

[†]E-mail: lyxiao@ustb.edu.cn

such as $\Sigma_b \bar{K}$ molecular [52–54] and dynamically generated state [55]. For the $\Xi_b(6100)^-$ and most recently observed $\Xi_b(6095)^0$ states, we can tentatively assign them to be the isospin doublet by considering the quarks constituents and mass difference. Currently, the vast majority of theoretical work interprets the two states as $1P$ -wave Ξ_b resonance with spin-parity $J^P = 3/2^-$ [37, 39, 42–44, 46, 48, 51, 56–59], but a very small number of studies suggest them may be $1P$ -wave Ξ_b resonance with spin-parity $J^P = 1/2^-$ [45]. For the other most recently reported state $\Xi_b(6087)^0$, the theoretical work interprets this state as $1P$ -wave Ξ_b baryon with spin-parity $J^P = 1/2^-$ [44, 46, 51, 57–59], which is inconsistent with the suggested spin-parity $J^P = 3/2^-$ from Particle Data Group [14]. The more theoretical studies with more references can be found in review articles [60, 61].

According to the predicted spectra of the Ξ_b and Ξ'_b baryons [19, 28, 37, 42, 50, 62–65], the mass distribution of the observed excited-state candidates lies between the predicted masses of the $1P$ -, $1D$ -, and $2S$ -wave states. In our previous works [40, 41], we have systematically studied the decay properties of the $1D$ -wave $\Xi_b^{(\prime)}$ baryons and given our theoretical explanations for the $\Xi_b(6327)^0$ and $\Xi_b(6333)^0$ states. In the present work, we carry out a systematical study of the $1P$ - and $2S$ -wave $\Xi_b^{(\prime)}$ states for both λ - and ρ -mode excitations with the quark pair creation(QPC) model. Meanwhile, we also include the chiral quark model's predictions for comparison. Through studies of their strong decay properties, we attempt to clarify the internal structure of the controversial excited states: $\Xi_b(6087)^0$, $\Xi_b(6095)^0/\Xi_b(6100)^-$, and $\Xi_b(6227)^{0,-}$. The quark model classification and Okubo-Zweig-Iizuka(OZI) allowed two-body decay modes are collected in Table II.

This paper is structured as follows. In Sec. II, we briefly introduce the QPC model, chiral quark model and the relationship of states in different coupling schemes. Then we present our numerical results and discussions in Sec. III. A summary is given in Sec. IV.

II. THEORETICAL FRAMEWORK

A. QPC model

The QPC model was first proposed by Micu [66], Car-litz and Kislinger [67], and further developed by the Orsay group [68–70]. According to this model, the strong decay takes place via the creation of quark-antiquark pair from the vacuum with quantum number 0^{++} . For a baryon decay process, one created quark regroups with two of the initial baryon state $|A\rangle$ to form a daughter baryon $|B\rangle$, and the created antiquark regroups with the other one quark to form a meson $|C\rangle$.

Within the QPC model, the transition operator for the two-body decay process $A \rightarrow BC$ in the nonrelativistic limit is

TABLE I: Masses and decay widths of the Ξ_b baryons from the Particle Data Group [14]. The unit is MeV.

State	J^P	Mass & Width	Status
Ξ_b^-	$1/2^+$	$M=5797.0 \pm 0.4$	***
Ξ_b^0	$1/2^+$	$M=5791.7 \pm 0.4$	***
$\Xi'_b(5935)^-(\Xi'_b^-)$	$1/2^+$	$M=5934.9 \pm 0.4$ $\Gamma = 0.03 \pm 0.032$	***
$\Xi_b(5945)^0(\Xi_b^{*0})$	$3/2^+$	$M=5952.3 \pm 0.6$ $\Gamma = 0.87 \pm 0.07$	***
$\Xi_b(5955)^-(\Xi_b^{*-})$	$3/2^+$	$M=5955.5 \pm 0.4$ $\Gamma = 1.43 \pm 0.11$	***
$\Xi_b(6087)^0$	$3/2^-$	$M=6087.0 \pm 0.5$ $\Gamma = 2.4 \pm 0.5$	***
$\Xi_b(6095)^0$	$3/2^-$	$M=6095.1 \pm 0.4$ $\Gamma = 0.50 \pm 0.35$	***
$\Xi_b(6100)^-$	$3/2^-$	$M=6099.8 \pm 0.4$ $\Gamma = 0.94 \pm 0.31$	***
$\Xi_b(6227)^-$	$?^?$	$M=6227.9 \pm 0.9$ $\Gamma = 19.9 \pm 2.6$	***
$\Xi_b(6227)^0$	$?^?$	$M=6226.8 \pm 1.6$ $\Gamma = 19_{-4}^{+5}$	***
$\Xi_b(6327)^0$	$?^?$	$M=6327.28 \pm 0.35$ $\Gamma < 2.56$	***
$\Xi_b(6333)^0$	$?^?$	$M=6332.69 \pm 0.28$ $\Gamma < 1.92$	***

given by

$$T = -3\gamma \sum_m \langle 1m; 1-m | 00 \rangle \int d^3 \mathbf{p}_4 d^3 \mathbf{p}_5 \delta^3(\mathbf{p}_4 + \mathbf{p}_5) \times \mathcal{Y}_1^m \left(\frac{\mathbf{p}_4 - \mathbf{p}_5}{2} \right) \chi_{1-m}^{45} \phi_0^{45} \omega_0^{45} a_{4i}^\dagger(\mathbf{p}_4) b_{5j}^\dagger(\mathbf{p}_5). \quad (1)$$

The dimensionless parameter γ accounts for the vacuum pair-production strength. \mathbf{p}_4 and \mathbf{p}_5 are the three-vector momenta of the created quark pair. $\mathcal{Y}_1^m = |\mathbf{p}| Y_1^m(\theta_p \phi_p)$ is solid harmonic polynomial and reflects the momentum-space distribution. χ_{1-m}^{45} , $\phi_0^{45} = (u\bar{u} + d\bar{d} + s\bar{s})/\sqrt{3}$, and $\omega_0^{45} = \delta_{ij}$ are the spin triplet, flavor function, and color singlet, respectively. $a_{4i}^\dagger d_{5j}^\dagger$ is the creation operator and denotes the quark pair-creation in the vacuum.

Describing the spatial wave functions of baryons and mesons with simple harmonic oscillator wave functions in momentum space, then we can obtain the partial decay amplitude in the center of mass frame,

$$\begin{aligned} & \mathcal{M}^{M_{J_A} M_{J_B} M_{J_C}}(A \rightarrow BC) \\ &= \gamma \sqrt{8E_A E_B E_C} \prod_{A,B,C} \langle \chi_{S_B M_{S_B}}^{124} \chi_{S_C M_{S_C}}^{35} \chi_{S_A M_{S_A}}^{123} \chi_{1-m}^{45} \rangle \\ & \quad \langle \varphi_B^{124} \varphi_C^{35} | \varphi_A^{123} \varphi_0^{45} \rangle I_{M_{L_B}, M_{L_C}}^{M_{L_A}, m}(\mathbf{p}). \end{aligned} \quad (2)$$

Here, $I_{M_{L_B}, M_{L_C}}^{M_{L_A}, m}(\mathbf{p})$ is the spatial integration. $\prod_{A,B,C}$ denotes the

TABLE II: Predicted mass of Ξ'_b and Ξ_b baryons(1P- and 2S-wave) in various quark models and possible OZI-allowed two body decay modes.

Notation	Quantum Number							Predicted Mass					Decay mode		
	n_λ	n_ρ	l_λ	l_ρ	L	s_ρ	j	J^P	GIM[42]	hCQM[37]	NQM[51]	RQM[19]	HM[39]	RFTM[45]	
$\Xi_b J^P = \frac{1}{2}^-, 1\rangle_\lambda$	0	0	1	0	1	0	1	$\frac{1}{2}^-$	6084		6077	6120	6079	6112	$\Xi_b^{(*)}\pi$
$\Xi_b J^P = \frac{3}{2}^-, 1\rangle_\lambda$	0	0	1	0	1	0	1	$\frac{3}{2}^-$	6097		6084	6130	6085	6126	
$\Xi_b J^P = \frac{1}{2}^-, 0\rangle_\rho$	0	0	0	1	1	1	0	$\frac{1}{2}^-$		6137	6243		6248		$\Xi_b\pi, \Xi_b^{(*)}\pi, \Xi_b(1P_\lambda)\pi, \Lambda_b\bar{K}$
$\Xi_b J^P = \frac{1}{2}^-, 1\rangle_\rho$	0	0	0	1	1	1	1	$\frac{1}{2}^-$		6138	6258		6271		
$\Xi_b J^P = \frac{3}{2}^-, 1\rangle_\rho$	0	0	0	1	1	1	1	$\frac{3}{2}^-$		6135	6249		6255		
$\Xi_b J^P = \frac{3}{2}^-, 2\rangle_\rho$	0	0	0	1	1	1	2	$\frac{3}{2}^-$		6136	6265		6277		
$\Xi_b J^P = \frac{5}{2}^-, 2\rangle_\rho$	0	0	0	1	1	1	2	$\frac{5}{2}^-$		6133	6276		6287		
$\Xi'_b J^P = \frac{1}{2}^-, 0\rangle_\lambda$	0	0	1	0	1	1	0	$\frac{1}{2}^-$	6238	6235	6201	6233	6198	6185	$\Xi_b\pi/\eta, \Xi_b^{(*)}\pi, \Xi_b(1P_\lambda)\pi, \Sigma_b^{(*)}K, \Lambda_b\bar{K}$
$\Xi'_b J^P = \frac{1}{2}^-, 1\rangle_\lambda$	0	0	1	0	1	1	1	$\frac{1}{2}^-$	6232	6237	6216	6227	6220	6220	
$\Xi'_b J^P = \frac{3}{2}^-, 1\rangle_\lambda$	0	0	1	0	1	1	1	$\frac{3}{2}^-$	6240	6232	6207	6234	6204	6242	
$\Xi'_b J^P = \frac{3}{2}^-, 2\rangle_\lambda$	0	0	1	0	1	1	2	$\frac{3}{2}^-$	6229	6234	6223	6224	6226	6326	
$\Xi'_b J^P = \frac{5}{2}^-, 2\rangle_\lambda$	0	0	1	0	1	1	2	$\frac{5}{2}^-$	6243	6229	6234	6226	6237	6339	
$\Xi'_b J^P = \frac{1}{2}^-, 1\rangle_\rho$	0	0	0	1	1	0	1	$\frac{1}{2}^-$		6366		6367			$\Xi_b^{(*)}\pi, \Sigma_b^{(*)}K, \Xi_b'(1P_\lambda)\pi$
$\Xi'_b J^P = \frac{3}{2}^-, 1\rangle_\rho$	0	0	0	1	1	0	1	$\frac{3}{2}^-$		6373		6374			
$\Xi_b J^P = \frac{1}{2}^+, 0\rangle_\lambda$	1	0	0	0	0	0	0	$\frac{1}{2}^+$	6224	6208		6266	6360	6276	$\Xi_b^{(*)}\pi, \Sigma_b^{(*)}K, \Xi_b'(1P_\lambda)\pi$
$\Xi_b J^P = \frac{1}{2}^+, 0\rangle_\rho$	0	1	0	0	0	0	0	$\frac{1}{2}^+$				6699			$\Xi_b^{(*)}\pi, \Sigma_b^{(*)}K, \Xi_b'(1P_\lambda)\pi, \Xi_b(1P_\rho)\pi, \Sigma_b(1P_\lambda)\Lambda_b(1P_\rho)\bar{K}, \Xi_b'(1D_{\lambda\lambda/\rho\rho})\pi$
$\Xi'_b J^P = \frac{1}{2}^+, 1\rangle_\lambda$	1	0	0	0	0	1	1	$\frac{1}{2}^+$	6350	6328		6329	6479	6367	$\Xi_b\pi, \Xi_b^{(*)}\pi, \Sigma_b^{(*)}K, \Lambda_b\bar{K}, \Xi_b^{(*)}\eta, \Lambda/\Sigma B, \Xi_b(1P_\lambda)\pi, \Xi_b'(1P_\lambda)\pi, \Lambda_b(1P_\lambda)\bar{K}, \Sigma_b/\Omega_b(1P_\lambda)K, \Sigma_b(1P_\rho)K, \Xi_b^{(*)}(1D_{\lambda\lambda/\rho\rho})\pi, \Lambda_b(1D_{\lambda\lambda/\rho\rho})\bar{K}, \Sigma_b(1D_{\lambda\lambda})K$
$\Xi'_b J^P = \frac{3}{2}^+, 1\rangle_\lambda$	1	0	0	0	0	1	1	$\frac{3}{2}^+$	6370	6343		6342	6508	6371	
$\Xi'_b J^P = \frac{1}{2}^+, 1\rangle_\rho$	0	1	0	0	0	1	1	$\frac{1}{2}^+$			6818			$\Xi_b\pi/\eta, \Xi_b^{(*)}\pi/\eta, \Sigma_b^{(*)}K, \Lambda_b\bar{K}, \Lambda/\Sigma B, \Xi_b(1P_{\lambda/\rho})\pi/\eta, \Xi_b'(1P_\lambda)\pi/\eta, \Xi_b'(1P_\rho)\pi, \Lambda_b(1P_{\lambda/\rho})\bar{K}, \Sigma_b/\Omega_b(1P_\lambda)K, \Sigma_b(1P_\rho)K, \Xi_b^{(*)}(1D_{\lambda\lambda/\rho\rho})\pi, \Lambda_b(1D_{\lambda\lambda/\rho\rho})\bar{K}, \Sigma_b(1D_{\lambda\lambda})K$	
$\Xi'_b J^P = \frac{3}{2}^+, 1\rangle_\rho$	0	1	0	0	0	1	1	$\frac{3}{2}^+$					6847		

Clebsch-Gorden coefficients and reads

$$\sum \langle L_B M_{L_B}; S_B M_{S_B} | J_B, M_{J_B} \rangle \langle L_C M_{L_C}; S_C M_{S_C} | J_C, M_{J_C} \rangle \quad (3)$$

$$\times \langle L_A M_{L_A}; S_A M_{S_A} | J_A, M_{J_A} \rangle \langle 1m; 1-m | 00 \rangle.$$

As in our previous work [71], we modify the vertex by introducing a form factor from the literature [72–74] to account for its overly hard behavior at high momenta within the quark pair creation model. To address this, we introduce a form factor, which imparts a finite-size character to the quark-pair-creation vertex, moving beyond the point-like description. It reads

$$\mathcal{M}^{M_{J_A} M_{J_B} M_{J_C}}(A \rightarrow BC) \rightarrow \mathcal{M}^{M_{J_A} M_{J_B} M_{J_C}}(A \rightarrow BC) e^{-\frac{\mathbf{p}^2}{2\Lambda^2}}. \quad (4)$$

In the equation, we fix the cut-off parameter $\Lambda = 780$ MeV, the same value as used in Ref. [75].

Finally, the decay width of the process $A \rightarrow BC$ can be obtained by the following formula,

$$\Gamma(A \rightarrow BC) = \pi^2 \frac{|\mathbf{p}|}{M_A^2} \frac{1}{2J_A + 1} \sum_{M_{J_A}, M_{J_B}, M_{J_C}} |\mathcal{M}^{M_{J_A}, M_{J_B}, M_{J_C}}|^2. \quad (5)$$

Where \mathbf{p} denotes the momentum of the daughter baryon $|B\rangle$ in the center of mass frame of baryon $|A\rangle$, its calculation is given by the following formula:

$$|\mathbf{p}| = \frac{\sqrt{[M_A^2 - (M_B - M_C)^2][M_A^2 - (M_B + M_C)^2]}}{2M_A}. \quad (6)$$

In this work, the values of the constituent quark mass, harmonic oscillator strength, vacuum pair-production strength are the same as in our previous article [41].

B. Chiral quark model

In the framework of the chiral quark model (ChQM), the low energy effective quark-pseudoscalar-meson coupling at tree level in the SU(3) flavor basis reads [76]

$$\mathcal{L}_m = \sum_j \frac{\delta}{\sqrt{2}f_m} \bar{\psi}_j \gamma_\mu \gamma_5 \psi_j \vec{I} \cdot \partial^\mu \vec{\phi}_m. \quad (7)$$

In the equation, f_m denotes the pseudoscalar meson decay constant, and δ is a global parameter accounting for the

strength of the quark-pseudoscalar-meson couplings. ψ_j represents the j -th quark field in a baryon. I and ϕ_m denote an isospin operator and the pseudoscalar meson octet, respectively. Considering the harmonic oscillator spatial wave function of baryons being nonrelativistic form, the coupling is adopt the nonrelativistic form as well and is written as [75, 77, 78]

$$H_I = \mathcal{H}^{NR} + \mathcal{H}^{RC}, \quad (8)$$

with

$$\mathcal{H}^{NR} = g \sum_j \left(\mathcal{G} \boldsymbol{\sigma}_j \cdot \mathbf{q} + \frac{\omega_m}{2\mu_q} \boldsymbol{\sigma}_j \cdot \mathbf{p}_j \right) F(\mathbf{q}^2) I_j \varphi_m, \quad (9)$$

and

$$\begin{aligned} \mathcal{H}^{RC} = & -\frac{g}{32\mu_q^2} \sum_j \left[m^2 (\boldsymbol{\sigma}_j \cdot \mathbf{q}) \right. \\ & \left. + 2\boldsymbol{\sigma}_j \cdot (\mathbf{q} - 2\mathbf{p}_j) \times (\mathbf{q} \times \mathbf{p}_j) \right] F(\mathbf{q}^2) I_j \varphi_m. \end{aligned} \quad (10)$$

In the above equation, $\boldsymbol{\sigma}_j$ and \mathbf{p}_j are the spin operator and internal momentum operator of the j -th light quark within a hadron. \mathbf{q} , ω_m , φ_m and m are the three momentum, energy, plane wave, and mass of the final emitted pseudoscalar light meson, respectively. The reduced mass μ_q is expressed as $1/\mu_q = 1/m_j + 1/m'_j$ for the masses of the j -th quark in the initial and final baryons. The factor $F(\mathbf{q}^2) = \sqrt{\frac{\Lambda^2}{\Lambda^2 + \mathbf{q}^2}}$ is introduced to suppress the unphysical contributions in high momentum region. I_j is the isospin operator. g and \mathcal{G} are defined by $g = \delta \sqrt{(E_i + M_i)(E_f + M_f)}$ and $\mathcal{G} = -(\frac{\omega_m}{E_f + M_f} + 1 + \frac{\omega_m}{2m'_j})$, respectively. Here, $(E_{i/f}, M_{i/f})$ are the energy and mass of the initial/final baryon.

Within the ChQM, the strong decay amplitude for the $A(\text{initial baryon}) \rightarrow B(\text{final baryon}) + C(\text{final meson})$ process can be obtained with

$$\mathcal{M}(A \rightarrow BC) = \langle B | H_I | A \rangle. \quad (11)$$

Then, the partial decay width can be worked out by

$$\Gamma = \frac{1}{8\pi} \frac{|\mathbf{q}|}{M_i^2} \frac{1}{2J_i + 1} \sum_{J_{iz}, J_{fz}} |M_{J_{iz}, J_{fz}}|^2. \quad (12)$$

Here, J_i is the total angular momentum quantum number of the initial baryon. J_{iz} and J_{fz} are the third components of the total angular momenta of the initial and final baryons, respectively.

In the calculations, the constituent quark mass and harmonic oscillator strength are the same as in that of the QPC model. The other model parameters are the same as in Refs. [75, 77, 78]. It should be mentioned that the strong decay properties of the excited Ξ_b and Ξ'_b baryons have been studied within the QPC model [36, 38, 39, 48] and ChQM [15, 49]. However, in these works, the QPC model does not account for high-momentum corrections, while the ChQM neglects relativistic correction term \mathcal{H}^{RC} . To enhance the reliability of the results, we have incorporated the aforementioned corrections in this paper.

C. Coupling scheme

Due to the heavy quark symmetry, the physical states for the Ξ_b and Ξ'_b baryons may be closer to the j - j coupling scheme. In the heavy quark symmetry limit, the states within the j - j coupling scheme are constructed by

$$|J^P, j\rangle = \left| \{[(l_\rho l_\lambda)_L s_\rho]_j s_Q \} \right\rangle_{J^P}. \quad (13)$$

In the expression, l_ρ and l_λ are the quantum numbers of the orbital angular momentum for ρ - and λ -mode excitations, respectively. The the quantum number of total orbital angular momentum $L = |l_\rho - l_\lambda|, \dots, l_\rho + l_\lambda$. s_ρ is the spin quantum number of the light quark pair, and s_Q is the spin quantum number of the heavy quark.

Meanwhile, the states within the the j - j coupling scheme can be expressed as linear combinations of the states within the L - S coupling via [20]

$$\begin{aligned} \left| \{[(l_\rho l_\lambda)_L s_\rho]_j s_Q \} \right\rangle_{J^P} = & (-1)^{L+s_\rho+\frac{1}{2}+J} \sqrt{2J+1} \sum_S \sqrt{2S+1} \\ & \binom{L}{s_Q} \binom{s_\rho}{J} \binom{j}{S} \left| \{[(l_\rho l_\lambda)_L (s_\rho s_Q)_S]_J \} \right\rangle. \end{aligned} \quad (14)$$

The quantum number of total spin angular momentum $S = |s_\rho - s_Q|, \dots, s_\rho + s_Q$. J is the quantum number of total angular momentum.

III. CALCULATIONS AND RESULTS

We calculate the strong decays of $1P$ - and $2S$ -wave excited Ξ_b and Ξ'_b baryons within the j - j coupling scheme in the framework of the QPC model. Both λ -mode and ρ -mode excitations are considered in the present work. In addition, for a comparison we also give the decay properties of those Ξ_b and Ξ'_b excitations within the ChQM. It is anticipated that our theoretical calculations will not only shed light on the internal structure of the presently observed controversial states, but also provide a theoretical foundation for future experimental investigations of the "missing" resonances.

A. $1P$ -wave λ -mode excitations

For the $1P$ -wave λ -mode Ξ_b baryons, there are two states according to the quark model classification, which are $\Xi_b|J^P = 1/2^-, 1\rangle_\lambda$ and $\Xi_b|J^P = 3/2^-, 1\rangle_\lambda$. Their theoretical masses and possible two-body decay channels are listed in Table II. From the table, it is known that the predicted masses of the $1P$ -wave λ -mode Ξ_b baryons are about $M \simeq (6050-6150)$ MeV, and the possible two-body decay channels are $\Xi_b^{(*)}\pi$. Considering the uncertainty of the mass predictions, we plot the strong decay properties of the λ -mode $1P$ -wave Ξ_b states as a function of the mass in Fig. 1 with the QPC model.

It is obtained that the decay properties of $\Xi_b|J^P = 1/2^-, 1\rangle_\lambda$ and $\Xi_b|J^P = 3/2^-, 1\rangle_\lambda$ are sensitive to the masses. Meanwhile,

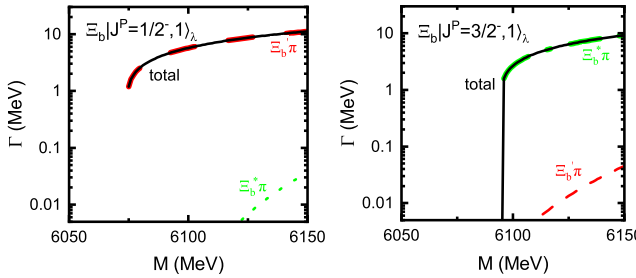


FIG. 1: Partial and total strong decay widths of the $1P$ -wave λ -mode Ξ_b excitations as functions of their masses.

TABLE III: The strong decay properties of the λ -mode $1P$ -wave Ξ_b states, which are taken as $\Xi_b(6087)^0$ and $\Xi_b(6095)^0$, respectively. Γ_{Total} represents the total decay width, and Expt. denotes the experimental value. The units are MeV.

Decay width	$\Xi_b J^P = \frac{1}{2}^-, 1\rangle_\lambda$		$\Xi_b J^P = \frac{3}{2}^-, 1\rangle_\lambda$	
	$\Xi_b(6087)^0$		$\Xi_b(6095)^0$	
	QPC	ChQM	QPC	ChQM
$\Gamma[\Xi'_b \pi^+]$	1.2	0.8	0.0	-
$\Gamma[\Xi_b^0 \pi^0]$	1.4	0.5	0.0	-
$\Gamma[\Xi_b^* \pi^+]$	0.0	-	0.1	0.1
$\Gamma[\Xi_b^0 \pi^0]$	0.0	-	0.9	0.3
Γ_{Total}	2.6	1.3	1.0	0.4
Expt.	2.4 ± 0.5		0.50 ± 0.35	

the two $1P$ -wave λ -mode Ξ_b baryons are probably very narrow states with a comparable total decay width of a few MeV. However, their main decay channels are completely different. The total decay width of $\Xi_b|J^P = 1/2^-, 1\rangle_\lambda$ is almost saturated by $\Xi'_b \pi$, while that of $\Xi_b|J^P = 3/2^-, 1\rangle_\lambda$ is almost saturated by $\Xi_b^* \pi$. Combining the measured masses and decay properties of the observed states $\Xi_b(6087)^0$ and $\Xi_b(6095)^0$, which mainly decay into $\Xi'_b \pi$ and $\Xi_b^* \pi$, respectively, $\Xi_b|J^P = 1/2^-, 1\rangle_\lambda$ and $\Xi_b|J^P = 3/2^-, 1\rangle_\lambda$ are good candidates of the two observed states. Hence, we further take $\Xi_b|J^P = 1/2^-, 1\rangle_\lambda$ and $\Xi_b|J^P = 3/2^-, 1\rangle_\lambda$ as $\Xi_b(6087)^0$ and $\Xi_b(6095)^0$, respectively, and collect their decay properties in Table III. For a comparison, we also studied the decay properties within the ChQM and listed the results in the same table as well.

Within the QPC model, the total decay width of $\Xi_b|J^P = 1/2^-, 1\rangle_\lambda$ is

$$\Gamma_{\text{Total}} \simeq 2.6 \text{ MeV}, \quad (15)$$

which is twice as large as that of the ChQM and highly consistent with the observation. Meanwhile, the dominant decay channels are $\Xi'_b \pi^+$ and $\Xi_b^0 \pi^0$. The corresponding branching fractions with the QPC model are

$$\frac{\Gamma[\Xi_b|J^P = 1/2^-, 1\rangle_\lambda \rightarrow \Xi'_b \pi^+]}{\Gamma_{\text{Total}}} \simeq 46\% \quad (16)$$

and

$$\frac{\Gamma[\Xi_b|J^P = 1/2^-, 1\rangle_\lambda \rightarrow \Xi_b^0 \pi^0]}{\Gamma_{\text{Total}}} \simeq 54\%, \quad (17)$$

respectively. This calculation is consistent with the fact that $\Xi_b(6087)^0$ was observed in $\Xi_b^0 \pi^- \pi^+$ final state mainly via the intermediate channel $\Xi'_b \pi^+$ by LHCb Collaboration [12]. In addition, if $\Xi_b(6087)^0$ corresponds to the state $\Xi_b|J^P = 1/2^-, 1\rangle_\lambda$ indeed, $\Xi_b(6087)^0 \rightarrow \Xi_b^0 \pi^0 \rightarrow \Xi_b^0 \pi^0 \pi^0$ may be another interesting decay chain for experimental exploration for the large predicted branching ratio of the $\Xi_b^0 \pi^0$ channel. However, this neutral decay channel will pose a challenge for experimental detection.

Our interpretations concur with prevailing theory in suggestion state $\Xi_b(6087)^0$ being a spin-parity $J^P = 1/2^-$ state, which directly contradicts the experimental value of $J^P = 3/2^-$. This discrepancy necessitates a careful experimental reassessment of the $\Xi_b(6087)^0$ state's spin-parity.

For the state $\Xi_b|J^P = 3/2^-, 1\rangle_\lambda$, the total decay width within the QPC model is

$$\Gamma_{\text{Total}} \simeq 1.0 \text{ MeV}, \quad (18)$$

which is close to the upper limit of the experimental value and approximately twice that of the ChQM. The main decay channels are $\Xi_b^* \pi^+$ and $\Xi_b^0 \pi^0$, and the corresponding branching ratios in the QPC model are

$$\frac{\Gamma[\Xi_b|J^P = 3/2^-, 1\rangle_\lambda \rightarrow \Xi_b^* \pi^+]}{\Gamma_{\text{Total}}} \simeq 10\% \quad (19)$$

and

$$\frac{\Gamma[\Xi_b|J^P = 1/2^-, 1\rangle_\lambda \rightarrow \Xi_b^0 \pi^0]}{\Gamma_{\text{Total}}} \simeq 90\%. \quad (20)$$

Considering the uncertainties for the experimental data and theoretical calculations, the decay properties of $\Xi_b|J^P = 3/2^-, 1\rangle_\lambda$ are consistent with those of $\Xi_b(6095)^0$. Additionally, due to the large branching ratio of decay channel $\Xi_b^0 \pi^0$, the $\Xi_b(6095)^0$ state are likely to be observed in the $\Xi_b^- \pi^+ \pi^0$ final state via the decay chain $\Xi_b(6095)^0 \rightarrow \Xi_b^0 \pi^0 \rightarrow \Xi_b^- \pi^+ \pi^0$, apart from the already experimentally observed decay channel $\Xi_b^0 \pi^- \pi^+$. It should be mentioned that the mass of $\Xi_b(6095)^0$ is very close to the threshold of $\Xi_b^* \pi$, and the partial decay widths are highly sensitive to the precision of mass.

As to the $1P$ -wave λ -mode Ξ'_b baryons, there are five states $\Xi'_b|J^P = 1/2^-, 0\rangle_\lambda$, $\Xi'_b|J^P = 1/2^-, 1\rangle_\lambda$, $\Xi'_b|J^P = 3/2^-, 1\rangle_\lambda$, $\Xi'_b|J^P = 3/2^-, 2\rangle_\lambda$, and $\Xi'_b|J^P = 5/2^-, 2\rangle_\lambda$. According to the theoretical predictions by various methods, the mass of the $1P$ -wave λ -mode Ξ'_b baryons is about $M \sim 6.23$ GeV (see table II). Based on the predicted masses, these states are probably assignments of observed state $\Xi_b(6227)$. Hence, the investigation of the properties of these states is crucial for clarifying the internal structure of the state $\Xi_b(6227)$. Considering the uncertainty of the mass predictions as well, we plot the decay properties of the $1P$ -wave λ -mode Ξ'_b baryons as functions of masses within the range of $M = (6150 - 6350)$ MeV within the QPC model, as shown in Fig. 2.

We can find that $\Xi'_b|J^P = 1/2^-, 0\rangle_\lambda$ is likely a moderate state with a decay width on the order of tens of MeV. The dominant decay channels are $\Lambda_b \bar{K}$ and $\Xi_b \pi$. For $\Xi'_b|J^P = 1/2^-, 1\rangle_\lambda$, its total decay width is about 20-30 MeV, and the dominant decay

TABLE IV: The strong decay properties of the λ -mode $1P$ -wave Ξ'_b states, which masses are taken from the predictions in Ref. [51]. Γ_{Total} represents the total decay width, and Expt. denotes the experimental value. The units are MeV.

Decay width	$\Xi'_b J^P = \frac{1}{2}^-, 0\rangle_\lambda$									
	$M = 6201$		$M = 6216$		$M = 6207$		$\Xi_b(6227)^0$		$\Xi_b(6227)^0$	
	QPC	ChQM	QPC	ChQM	QPC	ChQM	QPC	ChQM	QPC	ChQM
$\Gamma[\Xi_b\pi]$	41.8	24.2	0.0	0.0	0.0	0.0	4.6	5.5	4.6	5.5
$\Gamma[\Xi'_b\pi]$	0.0	0.0	30.7	15.3	0.1	0.2	0.4	0.5	0.2	0.3
$\Gamma[\Xi_b^*\pi]$	0.0	0.0	0.2	0.3	28.0	13.4	0.3	0.3	0.4	0.6
$\Gamma[\Lambda_b\bar{K}]$	53.2	22.2	0.0	0.0	0.0	0.0	2.3	1.9	2.3	2.9
$\Xi_b J^P = \frac{1}{2}^-, 1\rangle_\lambda \pi$	-	-	-	-	-	-	0.0	0.1	0.0	0.0
Γ_{Total}	95.0	46.4	30.9	15.6	28.1	13.6	7.6	8.3	7.5	9.3
Expt.										19^{+5}_{-4}

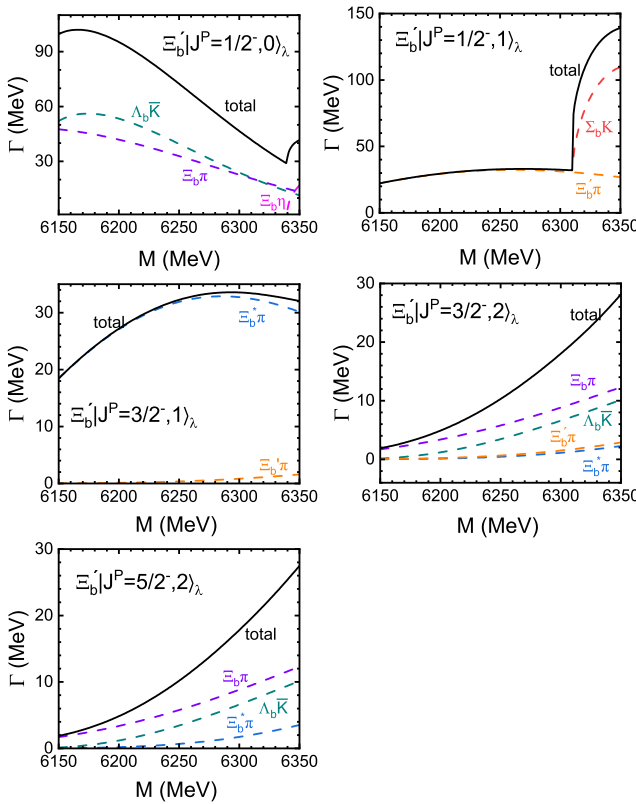


FIG. 2: Partial and total strong decay widths of the $1P$ -wave λ -mode Ξ'_b excitations as functions of their masses. Some decay channels are too small to show in figure.

channel is $\Xi'_b\pi$. However, we notice that if its mass lies above the $\Sigma_b K$ threshold, this mode becomes dominant and the total decay width can increase dramatically to well over 100 MeV. The total decay width of $\Xi'_b |J^P = 3/2^-, 1\rangle_\lambda$ is comparable to that of $\Xi'_b |J^P = 1/2^-, 1\rangle_\lambda$, both on the order of 20-30 MeV. While $\Xi'_b |J^P = 3/2^-, 1\rangle_\lambda$ mainly decays into $\Xi^*\pi$, which stands in sharp contrast to that of $\Xi'_b |J^P = 1/2^-, 1\rangle_\lambda$. Considering the relatively narrow width, $\Xi'_b |J^P = 3/2^-, 1\rangle_\lambda$ is highly likely to be observed in the $\Xi_b\pi\pi$ final state via the decay chain $\Xi'_b |J^P = 3/2^-, 1\rangle_\lambda \rightarrow \Xi^*\pi \rightarrow \Xi_b\pi\pi$. $\Xi'_b |J^P = 3/2^-, 2\rangle_\lambda$ and

$\Xi'_b |J^P = 5/2^-, 2\rangle_\lambda$ share similar decay properties. Specifically, both have total decay widths less than 30 MeV, and their dominant decay modes are $\Xi_b\pi$ and $\Lambda_b\bar{K}$. Based on the decay properties of the observed state $\Xi_b(6227)$, we cannot rule out the possibility that $\Xi_b(6227)$ could be a candidate of $\Xi'_b |J^P = 3/2^-, 2\rangle_\lambda$ or $\Xi'_b |J^P = 5/2^-, 2\rangle_\lambda$.

To better visualize the decay properties of the $1P$ -wave λ -mode Ξ'_b baryons, we further calculate their decay properties with the masses fixed at the predictions in Ref. [51] within both the QPC model and ChQM, except for the states $\Xi'_b |J^P = 3/2^-, 2\rangle_\lambda$ and $\Xi'_b |J^P = 5/2^-, 2\rangle_\lambda$, which masses are fixed at the physical mass of $\Xi_b(6227)^0$. The results are listed in Table IV.

According to the results of the QPC model, when $\Xi'_b |J^P = 3/2^-, 2\rangle_\lambda$ and $\Xi'_b |J^P = 5/2^-, 2\rangle_\lambda$ are treated as $\Xi_b(6227)^0$, both have a total width of about

$$\Gamma_{\text{Total}} \simeq 7.6 - 7.5 \text{ MeV}, \quad (21)$$

which is approximately (40-39)% of the experimental central value. While, within the ChQM, the total decay widths of the two states are

$$\Gamma_{\text{Total}} \simeq 8.3 - 9.3 \text{ MeV}, \quad (22)$$

which is approximately (44-49)% of the experimental central value. Additionally, both predominantly decay to $\Xi_b\pi$ (including $\Xi_b^0\pi^0$ and $\Xi_b^-\pi^+$) and $\Lambda_b\bar{K}$, and the branching fraction ratio in the QPC model is

$$\frac{\Gamma[\Xi'_b |J^P = 3(5)/2^-, 2\rangle_\lambda \rightarrow \Lambda_b\bar{K}]}{\Gamma[\Xi'_b |J^P = 3(5)/2^-, 2\rangle_\lambda \rightarrow \Xi_b\pi]} \simeq 0.5. \quad (23)$$

This value is highly consistent with the experimental measurement ($B(\Xi_b(6227)^- \rightarrow \Lambda_b K)/B(\Xi_b(6227)^- \rightarrow \Xi_b^0\pi^-) \simeq 1.0 \pm 0.5$) by the LHCb Collaboration [9]. Therefore, within theoretical uncertainties, $\Xi'_b |J^P = 3/2^-, 2\rangle_\lambda$ and $\Xi'_b |J^P = 5/2^-, 2\rangle_\lambda$ could still be candidate states for the observed state $\Xi_b(6227)^0$.

Additionally, we know that the state $\Xi'_b |J^P = 3/2^-, 2\rangle_\lambda$ in the $j - j$ coupling scheme is the linear combination of the configurations in the $L - S$ coupling scheme. That means $\Xi'_b |J^P = 3/2^-, 2\rangle_\lambda$ in the $j - j$ coupling scheme contains a mixing angle θ . Considering the heavy quark symmetry being not strictly true and slightly breaking in the Ξ'_b system, the

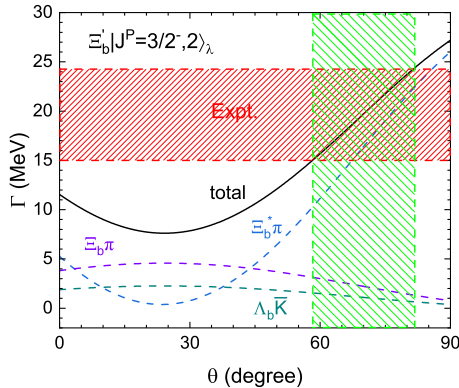


FIG. 3: Partial and total strong decay widths of $\Xi'_b|J^P = 3/2^-, 2\rangle_\lambda$ as a function of the mixing angle. Some decay channels are too small to show in figure.

mixing angle θ will fluctuate around the center value ($\theta \simeq 24^\circ$). To investigate this effect, we plot the strong decay properties of $\Xi'_b|J^P = 3/2^-, 2\rangle_\lambda$ within the QPC model as a function of the mixing angle varying in region of $\theta = (0^\circ - 90^\circ)$ in Fig. 3. As shown in the figure, when the mixing angle θ ranges from 58° to 81° , the total decay width of $\Xi'_b|J^P = 3/2^-, 2\rangle_\lambda$ is between 15 and 24 MeV, which is consistent with that of the observed state $\Xi_b(6227)^0$. Furthermore, considering the fact that $\Xi_b(6227)^0$ is observed in $\Xi_b^- \pi^+$ [10] and the experimental measured partial width ratio [9] of the decay channel $\Lambda_b \bar{K}$ to $\Xi_b \pi$ is approximately equal to one, selecting the lower limit of the allowed range for the mixing angle ($\theta \simeq 58^\circ$) is more appropriate. Under this condition, the branching ratios of decay channels $\Lambda_b \bar{K}$ and $\Xi_b \pi$ are approximately 11% and 21% respectively. Additionally, the decay channel $\Xi_b^* \pi$ will occupy a considerably large branching ratio of about 68%. Hence $\Xi_b \pi \pi$ could be another ideal observable channel for the state $\Xi_b(6227)^0$ via the decay chain $\Xi_b(6227) \rightarrow \Xi_b^* \pi \rightarrow \Xi_b \pi \pi$.

B. 1P-wave ρ -mode excitations

According to the symmetry of wave functions, there are five ρ -mode 1P-wave Ξ_b baryons (see Table II): $\Xi_b|J^P = 1/2^-, 0\rangle_\rho$, $\Xi_b|J^P = 1/2^-, 1\rangle_\rho$, $\Xi_b|J^P = 3/2^-, 1\rangle_\rho$, $\Xi_b|J^P = 3/2^-, 2\rangle_\rho$, and $\Xi_b|J^P = 5/2^-, 2\rangle_\rho$. As listed in Table II, the masses of these ρ -mode 1P-wave Ξ_b states fluctuate around $M \sim 6.25$ GeV. Firstly, we fix the masses at the predictions in Ref. [51], and study their strong decay properties within the QPC model and ChQM, as collected in Table V.

In the QPC model, the $\Xi_b|J^P = 1/2^-, 0\rangle_\rho$ may be a broad state with a total decay width of about $\Gamma \simeq 198$ MeV. The decay is governed by $\Xi_b \pi$ and $\Lambda_b \bar{K}$ with branching fractions

$$\frac{\Gamma[\Xi_b|J^P = 1/2^-, 0\rangle_\rho \rightarrow \Xi_b \pi]}{\Gamma_{\text{Total}}} \simeq 48\%, \quad (24)$$

$$\frac{\Gamma[\Xi_b|J^P = 1/2^-, 0\rangle_\rho \rightarrow \Lambda_b \bar{K}]}{\Gamma_{\text{Total}}} \simeq 52\%. \quad (25)$$

However, in the framework of ChQM, the $\Xi_b|J^P = 1/2^-, 0\rangle_\rho$ might be a moderate state with a width of $\Gamma \simeq 28$ MeV, which is about fifty times smaller than that predicted with the QPC model. The dominant decay channels become $\Xi_b^* \pi$ and $\Xi_b \pi$. The predicted branching fractions for the two mainly decay channels are 47% and 39%, respectively.

The states $\Xi_b|J^P = 1/2^-, 1\rangle_\rho$ and $\Xi_b|J^P = 3/2^-, 1\rangle_\rho$ are probably two moderate states with a comparable width of several tens of MeV. However, their dominant decay channels are different. For the $\Xi_b|J^P = 1/2^-, 1\rangle_\rho$, under the QPC model the primary decay channel is $\Xi_b^* \pi$, whereas under the ChQM the primary decay channels are $\Xi_b \pi$ and $\Lambda_b \bar{K}$. As to $\Xi_b|J^P = 3/2^-, 1\rangle_\rho$, its decay is almost saturated by the $\Xi_b^* \pi$ channel both the QPC model and ChQM. Hence the state may be observed experimentally in the $\Xi_b \pi \pi$ final state via the decay chain: $\Xi_b|J^P = 3/2^-, 1\rangle_\rho \rightarrow \Xi_b^* \pi \rightarrow \Xi_b \pi \pi$.

The other two 1P-wave ρ -mode states $\Xi_b|J^P = 3/2^-, 2\rangle_\rho$ and $\Xi_b|J^P = 5/2^-, 2\rangle_\rho$ are likely to be two narrow states, and their total decay widths are about ten to twenty MeV. Additionally, both of the two states decays dominantly via the channels $\Xi_b \pi$ and $\Lambda_b \bar{K}$. A comparison with the properties of the experimentally observed state $\Xi_b(6227)$ readily suggests that the states $\Xi_b|J^P = 3/2^-, 2\rangle_\rho$ and $\Xi_b|J^P = 5/2^-, 2\rangle_\rho$ are likely candidates for the state $\Xi_b(6227)$. Hence, we further take $\Xi_b|J^P = 3/2^-, 2\rangle_\rho$ and $\Xi_b|J^P = 5/2^-, 2\rangle_\rho$ as $\Xi_b(6227)^0$, and list their decay properties in Table V as well.

It is obtained that the ratio of the two primary decay channels $\Xi_b \pi$ and $\Lambda_b \bar{K}$ is

$$\frac{\Gamma[\Xi_b|J^P = 3(5)/2^-, 2\rangle_\lambda \rightarrow \Lambda_b \bar{K}]}{\Gamma[\Xi_b|J^P = 3(5)/2^-, 2\rangle_\lambda \rightarrow \Xi_b \pi]} \simeq 0.5, \quad (26)$$

which agrees well with the experimental value measured by the LHCb Collaboration [9]. The total decay width of $\Xi_b|J^P = 3/2^-, 2\rangle_\rho$ and $\Xi_b|J^P = 5/2^-, 2\rangle_\rho$ in the ChQM is about

$$\Gamma_{\text{Total}} \simeq 14.1 \text{ MeV}, \quad (27)$$

which is very close to the experimental lower limit. Hence, $\Xi_b|J^P = 3/2^-, 2\rangle_\rho$ and $\Xi_b|J^P = 5/2^-, 2\rangle_\rho$ might be good candidates for the $\Xi_b(6227)^0$. However, the decay properties of $\Xi_b|J^P = 3/2^-, 2\rangle_\rho$ and $\Xi_b|J^P = 5/2^-, 2\rangle_\rho$ are so similar that distinguishing them from each other would be very difficult both in experiment and theory.

Similarly, considering the uncertainty of the masses, we further investigate the strong decay widths of the 1P-wave ρ -mode Ξ_b states with the QPC model as a function of the mass varying in region of $M = (6100 - 6300)$ MeV in Fig. 4. It is shown that the decay properties of the five 1P-wave ρ -mode Ξ_b excitations exhibit a significant dependence on the mass across the defined range.

For the 1P-wave ρ -mode Ξ'_b excitations, there are two states $\Xi'_b|J^P = 1/2^-, 1\rangle_\rho$ and $\Xi'_b|J^P = 3/2^-, 1\rangle_\rho$. For their masses, there are some discussions in theoretical references and we have collected in Table II as well. From the table, the masses of the 1P-wave ρ -mode Ξ'_b baryons are about $M \sim 6.37$ GeV. Fixing their masses on the predictions in Ref. [51], we calculate their strong decay properties, and collect the results in Table VI.

TABLE V: The strong decay properties of the ρ -mode $1P$ -wave Ξ_b states, which masses are taken from the predictions in Ref. [51]. Γ_{Total} represents the total decay width, and Expt. denotes the experimental value. The units are MeV.

Decay width	$\Xi_b J^P = \frac{1}{2}^-, 0\rangle_\rho$		$\Xi_b J^P = \frac{1}{2}^-, 1\rangle_\rho$		$\Xi_b J^P = \frac{3}{2}^-, 1\rangle_\rho$		$\Xi_b J^P = \frac{3}{2}^-, 2\rangle_\rho$		$\Xi_b J^P = \frac{5}{2}^-, 2\rangle_\rho$	
	$M = 6243$		$M = 6258$		$M = 6249$		$M = 6265(\Xi_b(6227)^0)$		$M = 6276(\Xi_b(6227)^0)$	
	QPC	ChQM	QPC	ChQM	QPC	ChQM	QPC	ChQM	QPC	ChQM
$\Gamma[\Xi_b\pi]$	95.9	10.9	0.0	15.9	0.0	0.0	5.1(3.5)	12.3(8.5)	5.6(3.5)	13.5(8.5)
$\Gamma[\Xi'_b\pi]$	0.0	13.1	70.6	8.4	0.3	0.6	0.7(0.3)	1.5(0.7)	0.3(0.1)	0.8(0.3)
$\Gamma[\Xi_b^*\pi]$	0.0	0.0	0.4	1.1	66.6	59.5	0.5(0.2)	0.9(0.4)	0.9(0.3)	2.1(0.8)
$\Gamma[\Lambda_b\bar{K}]$	102.4	3.9	0.0	15.9	0.0	0.0	3.3(1.7)	8.2(4.5)	3.8(1.7)	9.4(4.5)
$\Gamma[\Xi_b J^P = \frac{1}{2}^-, 1\rangle_\lambda \pi]$	0.0	0.0	0.5	0.1	0.0	0.0	0.4(0.0)	0.1(0.0)	0.2(0.0)	0.0(0.0)
$\Gamma[\Xi_b J^P = \frac{3}{2}^-, 1\rangle_\lambda \pi]$	0.0	0.0	0.0	0.0	0.1	0.0	0.1(0.0)	0.0(0.0)	0.3(0.0)	0.2(0.0)
Γ_{Total}	198.3	27.9	71.5	41.4	67.0	60.2	10.1(5.7)	23.0(14.1)	11.1(5.6)	26.0(14.1)
Expt.										19^{+5}_{-4}

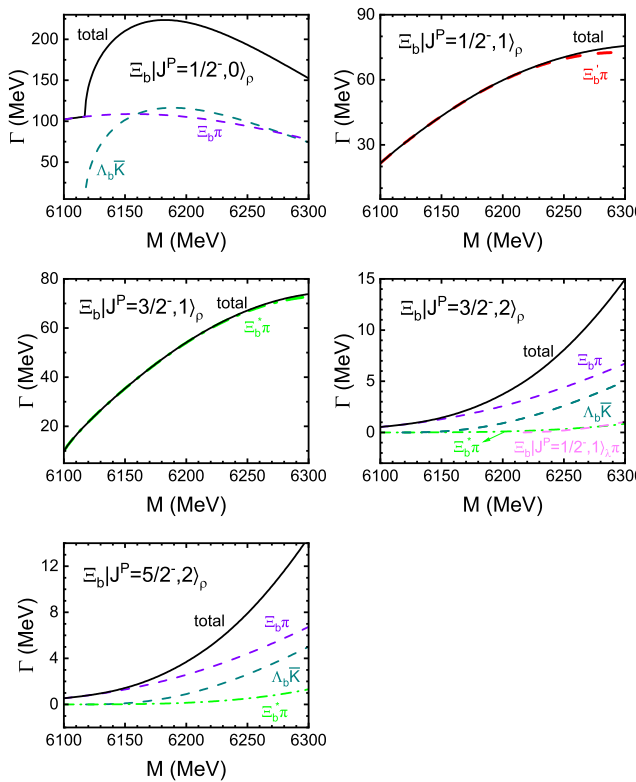


FIG. 4: Partial and total strong decay widths of the $1P$ -wave ρ -mode Ξ_b excitations as functions of their masses. Some decay channels are too small to show in figure.

Within the QPC model, the two states $\Xi'_b |J^P = 1/2^-, 1\rangle_\rho$ and $\Xi'_b |J^P = 3/2^-, 1\rangle_\rho$ are broad states with a width of $\Gamma \sim 150$ MeV. However, their dominant decay channels are different. For the state $\Xi'_b |J^P = 1/2^-, 1\rangle_\rho$, the mainly decay channel is $\Sigma_b K$, and the corresponding branching fractions can reach up to

$$\frac{\Gamma[\Xi'_b |J^P = 1/2^-, 1\rangle_\rho \rightarrow \Sigma_b K]}{\Gamma_{\text{Total}}} \simeq 74\%. \quad (28)$$

The large branching ratios indicate the state $\Xi'_b |J^P = 1/2^-, 1\rangle_\rho$

TABLE VI: The strong decay properties of the ρ -mode $1P$ -wave Ξ'_b states, which masses are taken from the predictions in Ref. [51]. Γ_{Total} represents the total decay width. The units are MeV.

Decay width	$\Xi'_b J^P = \frac{1}{2}^-, 1\rangle_\rho$		$\Xi'_b J^P = \frac{3}{2}^-, 1\rangle_\rho$	
	$M = 6366$		$M = 6373$	
	QPC	ChQM	QPC	ChQM
$\Gamma[\Xi'_b\pi]$	33.4	22.8	3.1	4.5
$\Gamma[\Xi_b^*\pi]$	4.7	6.9	36.8	26.8
$\Gamma[\Sigma_b K]$	112.4	56.2	1.4	2.2
$\Gamma[\Sigma_b^* K]$	0.8	1.4	109.0	56.7
$\Gamma[\Xi'_b J^P = \frac{1}{2}^-, 0\rangle_\lambda \pi]$	0.0	0.0	0.1	0.1
$\Gamma[\Xi'_b J^P = \frac{1}{2}^-, 1\rangle_\lambda \pi]$	0.0	0.0	0.0	0.1
$\Gamma[\Xi'_b J^P = \frac{3}{2}^-, 1\rangle_\lambda \pi]$	0.0	0.1	0.1	0.2
$\Gamma[\Xi'_b J^P = \frac{3}{2}^-, 2\rangle_\lambda \pi]$	0.0	0.0	0.0	0.0
$\Gamma[\Xi'_b J^P = \frac{5}{2}^-, 2\rangle_\lambda \pi]$	-	-	0.0	0.0
Γ_{Total}	151.3	87.4	150.5	90.6

is very likely be observed in the $\Lambda_b\pi K$ final state via the decay chain $\Xi'_b |J^P = 1/2^-, 1\rangle_\rho \rightarrow \Sigma_b K \rightarrow \Lambda_b\pi K$. Meanwhile, $\Xi'_b |J^P = 1/2^-, 1\rangle_\rho$ may have a sizeable decay rate into $\Xi'_b\pi$, and the predicted branching fraction is

$$\frac{\Gamma[\Xi'_b |J^P = 1/2^-, 1\rangle_\rho \rightarrow \Xi'_b\pi]}{\Gamma_{\text{Total}}} \simeq 22\%. \quad (29)$$

Hence, the $\Xi'_b |J^P = 1/2^-, 1\rangle_\rho$ may be observed in the $\Xi_b\pi\pi$ final state via the decay chain $\Xi'_b |J^P = 1/2^-, 1\rangle_\rho \rightarrow \Xi'_b\pi \rightarrow \Xi_b\pi\pi$.

While, for the other $1P$ -wave ρ -mode Ξ'_b excitation $\Xi'_b |J^P = 3/2^-, 1\rangle_\rho$, the dominant decay channel is $\Sigma_b^* K$, and the predicted branching fraction is

$$\frac{\Gamma[\Xi'_b |J^P = 3/2^-, 1\rangle_\rho \rightarrow \Sigma_b^* K]}{\Gamma_{\text{Total}}} \simeq 72\%. \quad (30)$$

Thus, the state $\Xi'_b |J^P = 3/2^-, 1\rangle_\rho$ may be observed in the $\Lambda_b\pi K$ final state via the decay chain $\Xi'_b |J^P = 3/2^-, 1\rangle_\rho \rightarrow \Sigma_b^* K \rightarrow \Lambda_b\pi K$. Moreover, the state $\Xi'_b |J^P = 3/2^-, 1\rangle_\rho$ have a

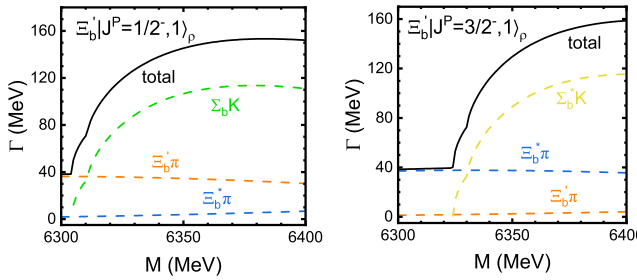


FIG. 5: Partial and total strong decay widths of the $1P$ -wave ρ -mode Ξ_b' excitations as functions of their masses. Some decay channels are too small to show in figure.

sizable decay rate into $\Xi_b^*\pi$ with a branching fraction of

$$\frac{\Gamma[\Xi_b' |J^P = 3/2^-, 1>_\rho \rightarrow \Xi_b^*\pi]}{\Gamma_{\text{Total}}} \simeq 24\%. \quad (31)$$

Therefore, the decay chain $\Xi_b' |J^P = 3/2^-, 1>_\rho \rightarrow \Xi_b^*\pi \rightarrow \Xi_b\pi\pi$ may be the other optional decay process to investigate the nature of $\Xi_b' |J^P = 3/2^-, 1>_\rho$.

For a comparison, the predicted results with the ChQM are collected in Table VI as well. It is found that the predicted main decay channels with the two models are agreement to each other, however, the predicted total decay widths with the QPC model are about 0.6 times larger than those with the ChQM.

We also plot the partial decay widths of the $1P$ -wave ρ -mode Ξ_b' excitations within the QPC model as a function of the mass in region of $M = (6300 - 6400)$ MeV. The sensitivities of the decay properties of two states to their masses are shown in Fig. 5. Within the masses varied in the region we considered in present work, the total decay widths of the $1P$ -wave ρ -mode Ξ_b' baryons are about $\Gamma \sim (40 - 160)$ MeV. We notice that the variation in the total width of $\Xi_b' |J^P = 1/2^-, 1>_\rho$ primarily stems from the mass dependence of its decay channel $\Sigma_b K$, while that of $\Xi_b' |J^P = 3/2^-, 1>_\rho$ primarily stems from the mass dependence of its decay channel $\Sigma_b^* K$.

C. $2S$ -wave λ -mode excitations

For the $2S$ -wave λ -mode Ξ_b baryons, there is only one state $\Xi_b |J^P = 1/2^+, 0>_\lambda$. According to the theoretical predictions by various methods, the mass of the $2S$ -wave λ -mode Ξ_b baryon is about $M \sim 6.26$ GeV. Fixing its mass at the prediction in Ref. [51], we calculate its strong decay properties with both the QPC model and ChQM, the theoretical results are listed in Table VII.

According to our calculations, the $\Xi_b |J^P = 1/2^+, 0>_\lambda$ is a very narrow state with a total decay width of only 3 to 4 MeV. The branching fractions of the mainly decay channels $\Xi_b'\pi$ and $\Xi_b^*\pi$ are

$$\frac{\Gamma[\Xi_b |J^P = 1/2^+, 0>_\lambda \rightarrow \Xi_b'\pi]}{\Gamma_{\text{Total}}} \simeq 37\%, \quad (32)$$

$$\frac{\Gamma[\Xi_b |J^P = 1/2^+, 0>_\lambda \rightarrow \Xi_b^*\pi]}{\Gamma_{\text{Total}}} \simeq 63\%. \quad (33)$$

Due to the narrow decay width, $\Xi_b |J^P = 1/2^+, 0>_\lambda$ has a high probability of being observed experimentally via the decay chain $\Xi_b |J^P = 1/2^+, 0>_\lambda \rightarrow \Xi_b'\pi / \Xi_b^*\pi \rightarrow \Xi_b\pi\pi$.

For the $2S$ -wave λ -mode Ξ_b' baryons, there are two states, which are $\Xi_b' |J^P = 1/2^+, 1>_\lambda$ and $\Xi_b' |J^P = 3/2^+, 1>_\lambda$. We have collected their theoretical masses and possible two-body decay channels in Table II. From the table, the masses of the $2S$ -wave λ -mode Ξ_b' baryons are about $M \sim 6.35$ GeV. Adopting the predicted masses from Ref. [51], we calculate their decay properties and list the theoretical results in Table VII as well.

Within the QPC model, the two $2S$ -wave λ -mode Ξ_b' excitations may be narrow states with a total decay widths of approximately a dozen MeV. The $\Xi_b' |J^P = 1/2^+, 1>_\lambda$ predominantly decays to $\Xi_b^*\pi$ and $\Xi_b |J^P = 1/2^-, 1>_\lambda\pi$. The branching fractions for the two mainly decay channels are

$$\frac{\Gamma[\Xi_b' |J^P = 1/2^+, 1>_\lambda \rightarrow \Xi_b^*\pi]}{\Gamma_{\text{Total}}} \simeq 30\%, \quad (34)$$

$$\frac{\Gamma[\Xi_b' |J^P = 1/2^+, 1>_\lambda \rightarrow \Xi_b |J^P = 1/2^-, 1>_\lambda\pi]}{\Gamma_{\text{Total}}} \simeq 27\%. \quad (35)$$

While, the decay of $\Xi_b' |J^P = 3/2^+, 1>_\lambda$ is governed by $\Xi_b |J^P = 3/2^-, 1>_\lambda\pi$ with branching fraction

$$\frac{\Gamma[\Xi_b' |J^P = 3/2^+, 1>_\lambda \rightarrow \Xi_b |J^P = 3/2^-, 1>_\lambda\pi]}{\Gamma_{\text{Total}}} \simeq 34\%. \quad (36)$$

Meanwhile, the decay channel $\Xi_b^*\pi$ also has a significant branching fraction, which is

$$\frac{\Gamma[\Xi_b' |J^P = 3/2^+, 1>_\lambda \rightarrow \Xi_b^*\pi]}{\Gamma_{\text{Total}}} \simeq 23\%. \quad (37)$$

The decay properties predicted by the ChQM for the $2S$ -wave λ -mode Ξ_b' states are somewhat different from those predicted by the QPC model. Within the ChQM, the total decay width of the $2S$ -wave λ -mode Ξ_b' states is about 0.4 times of that calculated by the QPC model. Meanwhile, the dominant decay channels of $\Xi_b' |J^P = 1/2^+, 1>_\lambda$ are $\Xi_b'\pi$ and $\Xi_b |J^P = 1/2^-, 1>_\lambda\pi$. And the mainly decay modes of $\Xi_b' |J^P = 3/2^+, 1>_\lambda$ are $\Xi_b^*\pi$ and $\Xi_b |J^P = 1/2^-, 1>_\lambda\pi$.

Considering the uncertainty of the masses of the $2S$ -wave λ -mode states, we further investigate the strong decay widths of the $2S$ -wave λ -mode states with the QPC model as a function of the mass in Fig. 6. The mass of the $2S$ -wave λ -mode Ξ_b state varies in the region of $M = (6200 - 6360)$ MeV, and those of the $2S$ -wave λ -mode Ξ_b' states vary in the region of $M = (6300 - 6500)$ MeV. From the figure, it is obtained that with the masses increasing the $\Sigma_b^* K$ becomes the dominant decay channel for the $2S$ -wave λ -mode Ξ_b' resonances. Meanwhile, the final state containing the $1P$ -wave charmed baryon will become more and more important as well.

TABLE VII: The strong decay properties of the λ -mode $2S$ -wave Ξ_b and Ξ'_b states, which masses are taken from the predictions in Ref. [51]. Γ_{Total} represents the total decay width. The units are MeV.

Decay width	$\Xi_b J^P = \frac{1}{2}^+, 0\rangle_\lambda$		$\Xi'_b J^P = \frac{1}{2}^+, 1\rangle_\lambda$		$\Xi'_b J^P = \frac{3}{2}^+, 1\rangle_\lambda$	
	$M = 6266$		$M = 6329$		$M = 6342$	
	QPC	ChQM	QPC	ChQM	QPC	ChQM
$\Gamma[\Xi_b\pi]$	-	-	1.5	0.3	1.3	0.3
$\Gamma[\Xi'_b\pi]$	1.5	1.0	2.6	1.5	0.7	0.4
$\Gamma[\Xi'_b\pi]$	2.6	1.7	5.0	0.7	3.3	1.8
$\Gamma[\Lambda_b\bar{K}]$	-	-	2.0	0.2	1.8	0.2
$\Gamma[\Sigma_bK]$	-	-	1.8	1.1	0.8	0.5
$\Gamma[\Sigma'_bK]$	-	-	-	-	1.4	0.9
$\Gamma[\Xi_b J^P = \frac{1}{2}^-, 1\rangle_\lambda \pi]$	-	-	4.8	2.5	0.2	1.1
$\Gamma[\Xi_b J^P = \frac{3}{2}^-, 1\rangle_\lambda \pi]$	-	-	0.2	0.3	5.0	0.7
Γ_{Total}	4.1	2.7	17.9	6.6	14.5	5.9

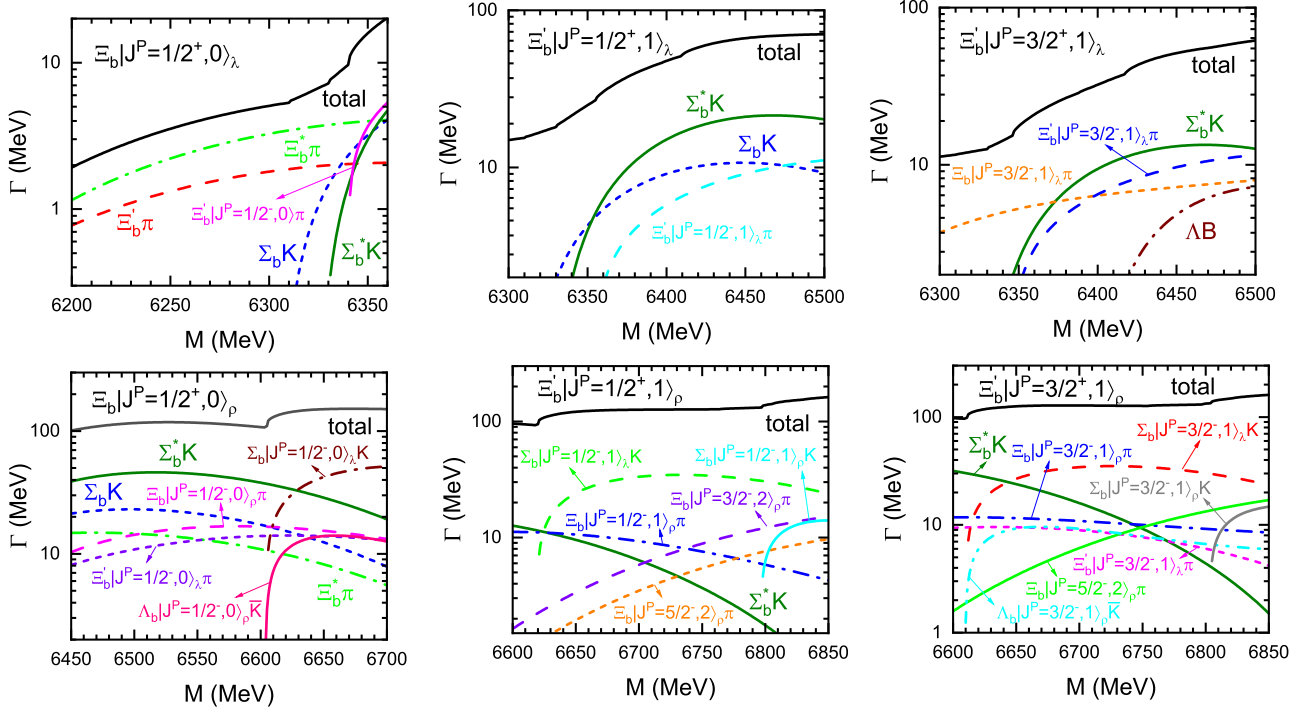


FIG. 6: Partial and total strong decay widths of the $2S$ -wave Ξ_b and Ξ'_b excitations as functions of their masses. Some decay channels are too small to show in figure.

D. $2S$ -wave ρ -mode excitations

For the $2S$ -wave ρ -mode Ξ_b baryons, there is only one state $\Xi_b |J^P = 1/2^+, 0\rangle_\rho$ as well according to the symmetry of the wave function. For its mass, there are a few discussions in theoretical references and we have collected in Table II. From the table, the mass of the $2S$ -wave ρ -mode Ξ_b baryon in Ref. [39] is about 6.70 GeV. While, a comparison between the Literature [39] and other studies regarding the calculated mass values for the $2S$ -wave λ -mode states reveals that Literature [39] overestimates the mass of the $2S$ -wave ρ -mode Ξ_b baryon by approximately 150 MeV. Hence, we fix the mass of

$\Xi_b |J^P = 1/2^+, 0\rangle_\rho$ at $M = 6549$ MeV, and collect its partial decay widths in Table VIII.

From the table, $\Xi_b |J^P = 1/2^+, 0\rangle_\rho$ has a total width of about $\Gamma \sim 117$ MeV, and mainly decays into $\Sigma_b^* K$. The corresponding branching fraction is

$$\frac{\Gamma[\Xi_b |J^P = 1/2^+, 0\rangle_\rho \rightarrow \Sigma_b^* K]}{\Gamma_{\text{Total}}} \simeq 38\%. \quad (38)$$

Meanwhile, the branching ratios to $\Sigma_b K$, $\Xi_b^* \pi$, $\Xi_b |J^P = 1/2^-, 0\rangle_\rho \pi$ and $\Xi'_b |J^P = 1/2^-, 0\rangle_\lambda \pi$ are also substantial, with values of 18%, 11%, 14%, and 11%, respectively.

However, according to the calculations within the ChQM,

TABLE VIII: The strong decay properties of the ρ -mode $2S$ -wave Ξ_b and Ξ'_b states, which masses are 150 MeV smaller than the predictions in Ref. [39]. Γ_{Total} represents the total decay width. The units are MeV.

Decay width	$\Xi_b J^P = \frac{1}{2}^+, 0\rangle_\rho$		$\Xi'_b J^P = \frac{1}{2}^+, 1\rangle_\rho$		$\Xi'_b J^P = \frac{3}{2}^+, 1\rangle_\rho$	
	$M = 6549$		$M = 6668$		$M = 6697$	
	QPC	ChQM	QPC	ChQM	QPC	ChQM
$\Gamma[\Xi_b \pi]$	-	-	0.5	0.0	0.2	0.0
$\Gamma[\Xi'_b \pi]$	6.2	3.8	4.1	3.6	0.8	0.6
$\Gamma[\Xi'_b \pi]$	13.2	8.5	2.4	10.7	4.7	3.9
$\Gamma[\Xi_b \eta]$	-	-	1.7	0.4	1.3	0.2
$\Gamma[\Xi'_b \eta]$	-	-	4.0	2.3	1.0	0.5
$\Gamma[\Xi'_b \eta]$	-	-	2.0	6.0	5.0	2.7
$\Gamma[\Lambda_b \bar{K}]$	-	-	0.1	0.8	0.0	1.1
$\Gamma[\Sigma_b K]$	21.3	3.6	14.3	1.5	2.7	0.1
$\Gamma[\Sigma'_b K]$	44.7	8.9	8.4	4.2	16.4	1.3
$\Gamma[\Lambda B]$	-	-	0.0	-	0.0	-
$\Gamma[\Sigma B]$	-	-	0.0	-	0.0	-
$\Gamma[\Sigma^* B]$	-	-	0.0	-	0.0	-
$\Gamma[\Xi B_s]$	-	-	-	-	0.0	-
$\Gamma[\Xi_b J^P = \frac{1}{2}^-, 1\rangle_\lambda \pi/\eta]$	-/-	-/-	3.1/1.6	49.7/12.3	0.5/0.0	0.9/0.0
$\Gamma[\Xi_b J^P = \frac{3}{2}^-, 1\rangle_\lambda \pi/\eta]$	-/-	-/-	1.1/0.0	1.9/0.0	3.2/2.0	4.9/20.6
$\Gamma[\Xi_b J^P = \frac{1}{2}^-, 0\rangle_\rho \pi]$	16.4	27.9	0.0	0.0	0.0	0.0
$\Gamma[\Xi_b J^P = \frac{1}{2}^-, 1\rangle_\rho \pi]$	0.0	0.0	10.2	20.7	1.7	3.6
$\Gamma[\Xi_b J^P = \frac{3}{2}^-, 1\rangle_\rho \pi]$	0.0	2.2	2.8	4.4	10.9	23.4
$\Gamma[\Xi_b J^P = \frac{3}{2}^-, 2\rangle_\rho \pi]$	0.8	0.0	4.2	9.5	2.8	6.2
$\Gamma[\Xi_b J^P = \frac{5}{2}^-, 2\rangle_\rho \pi]$	0.9	1.9	2.4	4.6	5.9	4.6
$\Gamma[\Xi'_b J^P = \frac{1}{2}^-, 0\rangle_\lambda \pi]$	12.9	1.7	0.0	0.0	0.0	0.0
$\Gamma[\Xi'_b J^P = \frac{1}{2}^-, 1\rangle_\lambda \pi]$	0.0	0.4	9.3	1.2	0.2	0.4
$\Gamma[\Xi'_b J^P = \frac{3}{2}^-, 1\rangle_\lambda \pi]$	0.0	2.7	0.4	0.0	9.0	1.6
$\Gamma[\Xi'_b J^P = \frac{3}{2}^-, 2\rangle_\lambda \pi]$	0.2	4.0	0.7	0.5	0.4	0.7
$\Gamma[\Xi'_b J^P = \frac{5}{2}^-, 2\rangle_\lambda \pi]$	0.3	0.5	0.4	0.7	0.9	1.5
$\Gamma[\Xi'_b J^P = \frac{1}{2}^-, 1\rangle_\rho \pi]$	-	-	5.4	9.7	0.9	1.6
$\Gamma[\Xi'_b J^P = \frac{3}{2}^-, 1\rangle_\rho \pi]$	-	-	0.9	5.3	6.3	11.7
$\Gamma[\Lambda_b J^P = \frac{1}{2}^-, 1\rangle_\lambda \bar{K}]$	-	-	3.3	16.7	0.6	0.2
$\Gamma[\Lambda_b J^P = \frac{3}{2}^-, 1\rangle_\lambda \bar{K}]$	-	-	1.2	0.5	3.4	4.4
$\Gamma[\Lambda_b J^P = \frac{1}{2}^-, 0\rangle_\rho \bar{K}]$	-	-	0.0	0.0	0.0	0.0
$\Gamma[\Lambda_b J^P = \frac{1}{2}^-, 1\rangle_\rho \bar{K}]$	-	-	9.3	18.8	0.4	1.0
$\Gamma[\Lambda_b J^P = \frac{3}{2}^-, 1\rangle_\rho \bar{K}]$	-	-	0.4	0.4	9.3	18.5
$\Gamma[\Lambda_b J^P = \frac{3}{2}^-, 2\rangle_\rho \bar{K}]$	-	-	0.4	1.4	0.6	1.8
$\Gamma[\Lambda_b J^P = \frac{5}{2}^-, 2\rangle_\rho \bar{K}]$	-	-	0.1	0.3	1.0	1.1
$\Gamma[\Sigma_b J^P = \frac{1}{2}^-, 0\rangle_\lambda K]$	-	-	0.0	0.0	0.0	0.0
$\Gamma[\Sigma_b J^P = \frac{1}{2}^-, 1\rangle_\lambda K]$	-	-	28.8	1.0	0.2	0.6
$\Gamma[\Sigma_b J^P = \frac{3}{2}^-, 1\rangle_\lambda K]$	-	-	0.2	0.0	34.1	1.3
$\Gamma[\Sigma_b J^P = \frac{3}{2}^-, 2\rangle_\lambda K]$	-	-	0.2	0.0	0.3	0.4
$\Gamma[\Sigma_b J^P = \frac{5}{2}^-, 2\rangle_\lambda K]$	-	-	0.1	0.1	0.5	0.4
$\Gamma[\Xi_b J^P = \frac{3}{2}^+, 2\rangle_{\lambda\lambda/\rho\rho} \pi]$	-/-	-/-	0.2/0.1	0.8/1.9	0.0/0.0	0.2/0.9
$\Gamma[\Xi_b J^P = \frac{5}{2}^+, 2\rangle_{\lambda\lambda/\rho\rho} \pi]$	-/-	-/-	0.0/0.0	25.6/0.0	0.2/0.1	1.2/4.6
$\Gamma[\Xi'_b J^P = \frac{1}{2}^+, 1\rangle_{\lambda\lambda} \pi]$	-	-	0.0	0.0	0.0	0.0
$\Gamma[\Xi'_b J^P = \frac{3}{2}^+, 1\rangle_{\lambda\lambda} \pi]$	-	-	0.0	0.1	0.0	0.0
$\Gamma[\Xi'_b J^P = \frac{3}{2}^+, 2\rangle_{\lambda\lambda} \pi]$	-	-	0.1	0.0	0.0	0.0
$\Gamma[\Xi'_b J^P = \frac{5}{2}^+, 2\rangle_{\lambda\lambda} \pi]$	-	-	0.0	1.3	0.2	0.0
$\Gamma[\Xi'_b J^P = \frac{5}{2}^+, 3\rangle_{\lambda\lambda} \pi]$	-	-	0.0	4.4	0.0	0.0
$\Gamma[\Xi'_b J^P = \frac{7}{2}^+, 3\rangle_{\lambda\lambda} \pi]$	-	-	0.0	0.0	0.0	4.9
$\Gamma[\Lambda_b J^P = \frac{3}{2}^+, 2\rangle_{\lambda\lambda} \bar{K}]$	-	-	-	-	0.0	0.0
$\Gamma[\Lambda_b J^P = \frac{5}{2}^+, 2\rangle_{\lambda\lambda} \bar{K}]$	-	-	-	-	0.2	0.0
Γ_{Total}	116.9	66.1	124.4	223.3	127.9	133.6

the total decay width of $\Xi_b|J^P = 1/2^+, 0\rangle_\rho$ is $\Gamma \simeq 66.1$ MeV, which is about 0.6 times of that predicted by the QPC model. Meanwhile, the dominant decay channel is $\Xi_b|J^P = 1/2^-, 0\rangle_\rho\pi$, and the branching fraction for this dominant decay channel is 42%.

As to the $2S$ -wave ρ -mode Ξ'_b baryons, there are two states: $\Xi'_b|J^P = 1/2^+, 1\rangle_\rho$ and $\Xi'_b|J^P = 3/2^+, 1\rangle_\rho$. Their theoretical masses and possible two-body decay channels are listed in Table II. We fix their masses at $M = 6668$ MeV and 6697 MeV, respectively. These values are 150 MeV smaller than the predictions in Ref. [39], and we collect their decay properties in Table VIII as well.

From the table, within the QPC model $\Xi'_b|J^P = 1/2^+, 1\rangle_\rho$ and $\Xi'_b|J^P = 3/2^+, 1\rangle_\rho$ have a comparable decay width of about $\Gamma \sim 120$ MeV. However, their dominant decay channels are different. $\Xi'_b|J^P = 1/2^+, 1\rangle_\rho$ decays predominantly to the $\Sigma_b|J^P = 1/2^-, 1\rangle_\lambda K$ channel, and the predicted branching fraction is

$$\frac{\Gamma[\Xi'_b|J^P = 1/2^+, 1\rangle_\rho \rightarrow \Sigma_b|J^P = 1/2^-, 1\rangle_\lambda K]}{\Gamma_{\text{Total}}} \simeq 23\%. \quad (39)$$

Furthermore, the $\Xi'_b|J^P = 1/2^+, 1\rangle_\rho$ state also decays to the $\Sigma_b K$ and $\Xi_b|J^P = 1/2^-, 1\rangle_\rho\pi$ channels with considerable branching ratios, which are about 11% and 8%, respectively.

For the $\Xi'_b|J^P = 3/2^+, 1\rangle_\rho$ state, its dominant decay channel is $\Sigma_b|J^P = 3/2^-, 1\rangle_\lambda K$. The branching fraction is predicted to be

$$\frac{\Gamma[\Xi'_b|J^P = 3/2^+, 1\rangle_\rho \rightarrow \Sigma_b|J^P = 3/2^-, 1\rangle_\lambda K]}{\Gamma_{\text{Total}}} \simeq 27\%. \quad (40)$$

Additionally, the branching ratios for the decays of the $\Xi'_b|J^P = 3/2^+, 1\rangle_\rho$ state to the $\Sigma_b^* K$ and $\Xi_b|J^P = 3/2^-, 1\rangle_\rho\pi$ channels are also sizable, at 13% and 9%, respectively.

However, within the ChQM, the total decay width of $\Xi'_b|J^P = 1/2^+, 1\rangle_\rho$ is about 100 MeV larger than the that of prediction via the QPC model. Furthermore, the dominant decay channel of $\Xi'_b|J^P = 1/2^+, 1\rangle_\rho$ is $\Xi_b|J^P = 1/2^-, 1\rangle_\lambda\pi$, with branching fraction being about 22%. As to the $\Xi'_b|J^P = 3/2^+, 1\rangle_\rho$ state, the total decay width calculated by the ChQM is comparable to that predicted by the QPC model. While, the main decay channels predicted by the two models are different. In the ChQM, the mainly channels for $\Xi'_b|J^P = 3/2^+, 1\rangle_\rho$ are $\Xi_b|J^P = 3/2^-, 1\rangle_\rho\pi$ and $\Xi_b|J^P = 3/2^-, 1\rangle_\lambda\pi$, with their respective branching ratios being 18% and 15%.

In addition, considering the uncertainty of the masses of the $2S$ -wave states, we further investigate the strong decay widths of $2S$ -wave Ξ_b and Ξ'_b states with the QPC model a function of the mass in Fig. 6. The mass of the $2S$ -wave ρ -mode Ξ_b state varies in the region of $M = (6450 - 6700)$ MeV, and those of the $2S$ -wave ρ -mode Ξ'_b states vary in the region of $M = (6600 - 6850)$ MeV. From the figure, we obtain that for the $2S$ -wave ρ -mode states, apart from ground states such as $\Sigma_b K$ and $\Sigma_b^* K$, the decay channels involving P -wave final states also play a significant role.

IV. SUMMARY

In this work, we systematically investigated the two-body strong decays of low-lying $1P$ - and $2S$ -wave Ξ_b and Ξ'_b excitations in the QPC model within the j - j coupling scheme. For a comparison, we also give our predictions within the chiral quark model. The main theoretical results are summarized as follows.

For the $1P$ -wave λ -mode Ξ_b states, $\Xi_b|J^P = 1/2^-, 1\rangle_\lambda$ is a very narrow state with a total decay width of about $\Gamma \simeq (1-2)$ MeV, and dominantly decays into the $\Xi'_b\pi$ channel. The other $1P$ -wave λ -mode Ξ_b state $\Xi_b|J^P = 3/2^-, 1\rangle_\lambda$ is likely a narrower state with a total decay width approximately half that of $\Xi_b|J^P = 1/2^-, 1\rangle_\lambda$. Its decay width is almost saturated by $\Xi_b^*\pi$. Combining the measured masses and decay properties of the observed states $\Xi_b(6087)$ and $\Xi_b(6095/6100)$, $\Xi_b|J^P = 1/2^-, 1\rangle_\lambda$ and $\Xi_b|J^P = 3/2^-, 1\rangle_\lambda$ are good candidates for the states $\Xi_b(6087)$ and $\Xi_b(6095/6100)$, respectively.

For the $1P$ -wave λ -mode Ξ'_b states, within the QPC model $\Xi'_b|J^P = 1/2^-, 0\rangle_\lambda$ is likely a moderate state with a decay width of $\Gamma \sim 95$ MeV. Meanwhile, the dominant channels are $\Lambda_b\bar{K}$ and $\Xi_b\pi$. The total widths of $\Xi'_b|J^P = 1/2^-, 1\rangle_\lambda$ and $\Xi'_b|J^P = 3/2^-, 1\rangle_\lambda$ are comparable in the QPC model, both in the range of $\Gamma \sim (20 - 30)$ MeV. However, their dominant decay channels are different. $\Xi'_b|J^P = 1/2^-, 1\rangle_\lambda$ mainly decays into $\Xi'_b\pi$, while $\Xi'_b|J^P = 3/2^-, 1\rangle_\lambda$ mainly decays into $\Xi_b^*\pi$. The dominant decay channels predicted by the ChQM for the three $1P$ -wave λ -mode states mentioned above are highly consistent with the predictions of the QPC model. However, the total decay width for the three states in the ChQM is about half of that in the QPC model. Both $\Xi'_b|J^P = 3/2^-, 2\rangle_\lambda$ and $\Xi'_b|J^P = 5/2^-, 2\rangle_\lambda$ have similar decay properties. They have large decay rates into the $\Xi_b\pi$ and $\Lambda_b\bar{K}$ channels. Their total decay width is close to 10 MeV, which is about half of the measured central value for the total width of the observed state $\Xi_b(6227)$. However, considering the theoretical uncertainties, $\Xi'_b|J^P = 3/2^-, 2\rangle_\lambda$ and $\Xi'_b|J^P = 5/2^-, 2\rangle_\lambda$ could still be considered as candidates for the state $\Xi_b(6227)$.

For the $1P$ -wave ρ -mode Ξ_b states, the decay properties of the two states $\Xi_b|J^P = 1/2^-, 0\rangle_\rho$ and $\Xi_b|J^P = 1/2^-, 1\rangle_\rho$ have a strong model dependency. In the QPC model, $\Xi_b|J^P = 1/2^-, 0\rangle_\rho$ has a broad width of $\Gamma \sim 198$ MeV, and mainly decays into the $\Xi_b\pi$ and $\Lambda_b\bar{K}$ channels. $\Xi_b|J^P = 1/2^-, 1\rangle_\rho$ may be a moderate state with a total decay width of $\Gamma \sim 72$ MeV. Its decay width is almost saturated by the $\Xi'_b\pi$ channel. However, in the ChQM, $\Xi_b|J^P = 1/2^-, 0\rangle_\rho$ is predicted to be a narrow state, and its decay is governed by the $\Xi'_b\pi$ and $\Xi_b\pi$ channels. $\Xi_b|J^P = 1/2^-, 1\rangle_\rho$ still have a moderate width, while the dominant decay channels are now the $\Xi_b\pi$ and $\Lambda_b\bar{K}$ channels. The state $\Xi_b|J^P = 3/2^-, 1\rangle_\rho$ dominantly decay into $\Xi_b^*\pi$, and probably has a moderate width of $\Gamma \sim 60$ MeV. $\Xi_b|J^P = 3/2^-, 2\rangle_\rho$ and $\Xi_b|J^P = 5/2^-, 2\rangle_\rho$ have similar decay properties, and mainly decay into $\Xi_b\pi$ and $\Lambda_b\bar{K}$. They are most likely to be narrow states with a comparable width of $\Gamma \sim 14$ MeV in the ChQM, which is about two times of that in the QPC model. Hence, $\Xi_b|J^P = 3/2^-, 2\rangle_\rho$ and $\Xi_b|J^P = 5/2^-, 2\rangle_\rho$ might be good candidates for the $\Xi_b(6227)$.

For the $1P$ -wave ρ -mode Ξ'_b states, within the QPC model $\Xi'_b|J^P = 1/2^-, 1\rangle_\rho$ and $\Xi'_b|J^P = 3/2^-, 1\rangle_\rho$ are broad states with a comparable width of $\Gamma \sim 151$ MeV. However, the dominant decay channel of $\Xi'_b|J^P = 1/2^-, 1\rangle_\rho$ is $\Sigma_b K$, and that of $\Xi'_b|J^P = 3/2^-, 1\rangle_\rho$ is $\Sigma_b^* K$. With the ChQM, the predicted main decay channels for the two $1P$ -wave ρ -mode Ξ'_b states are in agreement with the predictions in the QPC model. While, the total decay widths are about $\Gamma \sim (87 - 91)$ MeV, which are about 0.6 times smaller than those of calculated by the QPC model.

For the $2S$ -wave λ -mode Ξ_b state $\Xi_b|J^P = 1/2^+, 0\rangle_\lambda$, similar decay properties are predicted within the two models. $\Xi_b|J^P = 1/2^+, 0\rangle_\lambda$ may be a very narrow state with a total decay width of only 3 to 4 MeV, and has a high probability of being observed experimentally via the decay chain $\Xi_b|J^P = 1/2^+, 0\rangle_\lambda \rightarrow \Xi'_b \pi / \Xi_b^* \pi \rightarrow \Xi_b \pi \pi$.

For the $2S$ -wave λ -mode Ξ'_b states, their total decay widths are approximately a dozen MeV. $\Xi'_b|J^P = 1/2^+, 1\rangle_\lambda$ predominantly decays to $\Xi_b^* \pi$ and $\Xi_b|J^P = 1/2^-, 1\rangle_\lambda \pi$. While, $\Xi'_b|J^P = 3/2^+, 1\rangle_\lambda$ predominantly decays to $\Xi_b^* \pi$ and $\Xi_b|J^P = 3/2^-, 1\rangle_\lambda \pi$. However, within the ChQM, the total decay

widths of the two $2S$ -wave λ -mode Ξ'_b states are about 0.4 times of those predicted by the QPC model. Meanwhile, the dominant decay channels of $\Xi'_b|J^P = 1/2^+, 1\rangle_\lambda$ are $\Xi'_b \pi$ and $\Xi_b|J^P = 1/2^-, 1\rangle_\lambda \pi$. And the mainly decay modes of $\Xi'_b|J^P = 3/2^+, 1\rangle_\lambda$ are $\Xi_b^* \pi$ and $\Xi_b|J^P = 1/2^-, 1\rangle_\lambda \pi$.

As to the $2S$ -wave ρ -mode states, $\Xi_b|J^P = 1/2^+, 0\rangle_\rho$ has a total decay width of dozens to one hundred MeV. $\Xi'_b|J^P = 1/2^+, 1\rangle_\rho$ and $\Xi'_b|J^P = 3/2^+, 1\rangle_\rho$ may be two broad states, with a total decay width of over one hundred to two hundred MeV. Meanwhile, according to our calculations, in addition to decay channels $\Sigma_b^{(*)} K$ and $\Xi_b^* \pi$, two-body decay channels involving $1P$ -wave final states also play a significant role in experimental detection.

Acknowledgements

This work is supported by the National Natural Science Foundation of China under Grants No.12005013.

[1] Murray Gell-Mann. A Schematic Model of Baryons and Mesons. *Phys. Lett.*, 8:214–215, 1964.

[2] Eberhard Klempert and Jean-Marc Richard. Baryon spectroscopy. *Rev. Mod. Phys.*, 82:1095–1153, 2010.

[3] G. Zweig. An SU(3) model for strong interaction symmetry and its breaking. Version 1. 1 1964.

[4] T. Aaltonen et al. Observation and mass measurement of the baryon Xi_b^- . *Phys. Rev. Lett.*, 99:052002, 2007.

[5] T. Aaltonen et al. Observation of the Ξ_b^0 Baryon. *Phys. Rev. Lett.*, 107:102001, 2011.

[6] Serguei Chatrchyan et al. Observation of a new Ξ_b Baryon. *Phys. Rev. Lett.*, 108:252002, 2012.

[7] Roel Aaij et al. Observation of two new Ξ_b^- baryon resonances. *Phys. Rev. Lett.*, 114:062004, 2015.

[8] Roel Aaij et al. Measurement of the properties of the Ξ_b^0 baryon. *JHEP*, 05:161, 2016.

[9] Roel Aaij et al. Observation of a new Ξ_b^- resonance. *Phys. Rev. Lett.*, 121(7):072002, 2018.

[10] Roel Aaij et al. Observation of a new Ξ_b^0 state. *Phys. Rev. D*, 103(1):012004, 2021.

[11] Albert M Sirunyan et al. Observation of a New Excited Beauty Strange Baryon Decaying to $\Xi_b^- \pi^+ \pi^-$. *Phys. Rev. Lett.*, 126(25):252003, 2021.

[12] Roel Aaij et al. Observation of New Baryons in the $\Xi b - \pi^+ \pi^-$ and $\Xi b 0\pi^+ \pi^-$ Systems. *Phys. Rev. Lett.*, 131(17):171901, 2023.

[13] Roel Aaij et al. Observation of Two New Excited Ξ_b^0 States Decaying to $\Lambda_b^0 K^- \pi^+$. *Phys. Rev. Lett.*, 128(16):162001, 2022.

[14] S. Navas et al. Review of particle physics. *Phys. Rev. D*, 110(3):030001, 2024.

[15] Kai-Lei Wang, Ya-Xiong Yao, Xian-Hui Zhong, and Qiang Zhao. Strong and radiative decays of the low-lying S - and P -wave singly heavy baryons. *Phys. Rev. D*, 96(11):116016, 2017.

[16] Yohei Kawakami and Masayasu Harada. Singly heavy baryons with chiral partner structure in a three-flavor chiral model. *Phys. Rev. D*, 99(9):094016, 2019.

[17] Yonghee Kim, Yan-Rui Liu, Makoto Oka, and Kei Suzuki. Heavy baryon spectrum with chiral multiplets of scalar and vector diquarks. *Phys. Rev. D*, 104(5):054012, 2021.

[18] Bing Chen, Ke-Wei Wei, and Ailin Zhang. Assignments of Λ_Q and Ξ_Q baryons in the heavy quark-light diquark picture. *Eur. Phys. J. A*, 51:82, 2015.

[19] D. Ebert, R. N. Faustov, and V. O. Galkin. Spectroscopy and Regge trajectories of heavy baryons in the relativistic quark-diquark picture. *Phys. Rev. D*, 84:014025, 2011.

[20] W. Roberts and Muslema Pervin. Heavy baryons in a quark model. *Int. J. Mod. Phys. A*, 23:2817–2860, 2008.

[21] J. Vijande, A. Valcarce, T. F. Carames, and H. Garcilazo. Heavy hadron spectroscopy: a quark model perspective. *Int. J. Mod. Phys. E*, 22:1330011, 2013.

[22] Bing Chen, Si-Qiang Luo, Xiang Liu, and Takayuki Matsuki. Interpretation of the observed $\Lambda_b(6146)^0$ and $\Lambda_b(6152)^0$ states as $1D$ bottom baryons. *Phys. Rev. D*, 100(9):094032, 2019.

[23] Ya-Xiong Yao, Kai-Lei Wang, and Xian-Hui Zhong. Strong and radiative decays of the low-lying D -wave singly heavy baryons. *Phys. Rev. D*, 98(7):076015, 2018.

[24] Hua-Xing Chen, Qiang Mao, Atsushi Hosaka, Xiang Liu, and Shi-Lin Zhu. D -wave charmed and bottomed baryons from QCD sum rules. *Phys. Rev. D*, 94(11):114016, 2016.

[25] Ke-Wei Wei, Bing Chen, Na Liu, Qian-Qian Wang, and Xin-Heng Guo. Spectroscopy of singly, doubly, and triply bottom baryons. *Phys. Rev. D*, 95(11):116005, 2017.

[26] C. Garcia-Recio, J. Nieves, O. Romanets, L. L. Salcedo, and L. Tolos. Odd parity bottom-flavored baryon resonances. *Phys. Rev. D*, 87(3):034032, 2013.

[27] A. Valcarce, H. Garcilazo, and J. Vijande. Towards an understanding of heavy baryon spectroscopy. *Eur. Phys. J. A*, 37:217–225, 2008.

[28] D. Ebert, R. N. Faustov, and V. O. Galkin. Masses of excited heavy baryons in the relativistic quark model. *Phys. Lett. B*, 659:612–620, 2008.

[29] Elizabeth Ellen Jenkins. Model-Independent Bottom Baryon Mass Predictions in the $1/N(c)$ Expansion. *Phys. Rev. D*,

77:034012, 2008.

[30] Marek Karliner, Boaz Keren-Zur, Harry J. Lipkin, and Jonathan L. Rosner. The Quark Model and b Baryons. *Annals Phys.*, 324:2–15, 2009.

[31] H. Garcilazo, J. Vijande, and A. Valcarce. Faddeev study of heavy baryon spectroscopy. *J. Phys. G*, 34:961–976, 2007.

[32] Qiang Mao, Hua-Xing Chen, Wei Chen, Atsushi Hosaka, Xiang Liu, and Shi-Lin Zhu. QCD sum rule calculation for P-wave bottom baryons. *Phys. Rev. D*, 92(11):114007, 2015.

[33] Zhi-Gang Wang. Analysis of the $1/2^-$ and $3/2^-$ heavy and doubly heavy baryon states with QCD sum rules. *Eur. Phys. J. A*, 47:81, 2011.

[34] Zhen-Yang Wang, Jing-Juan Qi, Xin-Heng Guo, and Ke-Wei Wei. Spectra of charmed and bottom baryons with hyperfine interaction. *Chin. Phys. C*, 41(9):093103, 2017.

[35] Kaushal Thakkar, Zalak Shah, Ajay Kumar Rai, and P. C. Vinodkumar. Excited State Mass spectra and Regge trajectories of Bottom Baryons. *Nucl. Phys. A*, 965:57–73, 2017.

[36] Bing Chen, Ke-Wei Wei, Xiang Liu, and Ailin Zhang. Role of newly discovered $\Xi_b(6227)^-$ for constructing excited bottom baryon family. *Phys. Rev. D*, 98(3):031502, 2018.

[37] Amee Kakadiya, Zalak Shah, and Ajay Kumar Rai. Mass spectra and decay properties of singly heavy bottom-strange baryons. *Int. J. Mod. Phys. A*, 37(11n12):2250053, 2022.

[38] Roelof Bijker, Hugo García-Tecocoatzi, Alessandro Giachino, Emmanuel Ortiz-Pacheco, and Elena Santopinto. Masses and decay widths of Ξ_c/b and Ξ_c/b' baryons. *Phys. Rev. D*, 105(7):074029, 2022.

[39] H. García-Tecocoatzi, A. Giachino, A. Ramirez-Morales, Ailier Rivero-Acosta, E. Santopinto, and Carlos Alberto Vaquera-Araujo. Strong decay widths and mass spectra of the 1D, 2P and 2S singly bottom baryons. *Phys. Rev. D*, 110(11):114005, 2024.

[40] Wen-Jia Wang, Yu-Hui Zhou, Li-Ye Xiao, and Xian-Hui Zhong. 1D-wave bottom-strange baryons and possible interpretation of $\Xi_b(6327)^0$ and $\Xi_b(6333)^0$. *Phys. Rev. D*, 105(7):074008, 2022.

[41] Yu-Hui Zhou, Wen-Jia Wang, Li-Ye Xiao, and Xian-Hui Zhong. Strong decays of low-lying D-wave Ξ_b and Ξ_b' baryons with quark-pair creation model. *Phys. Rev. D*, 108(9):094032, 2023.

[42] Zhen-Yu Li, Guo-Liang Yu, Zhi-Gang Wang, Jian-Zhong Gu, Jie Lu, and Hong-Tao Shen. Systematic analysis of strange single heavy baryons and *. *Chin. Phys. C*, 47(7):073105, 2023.

[43] Xin-Zhen Weng, Wei-Zhen Deng, and Shi-Lin Zhu. Heavy baryons in the relativized quark model with chromodynamics. *Phys. Rev. D*, 110(5):056052, 2024.

[44] Roelof Bijker and Emmanuel Ortiz-Pacheco. Spectroscopy of heavy baryons. *Nuovo Cim. C*, 47(4):175, 2024.

[45] Pooja Jakhad, Juhí Oudichhya, and Ajay Kumar Rai. Interpretation of recently discovered single bottom baryons in the relativistic flux tube model. *Phys. Rev. D*, 110(9):094005, 2024.

[46] Zhen-Yu Li, Guo-Liang Yu, Zhi-Gang Wang, and Jian-Zhong Gu. Heavy quark dominance in orbital excitation of singly and doubly heavy baryons. *Eur. Phys. J. C*, 84(2):106, 2024.

[47] Zhen-Yu Li, Guo-Liang Yu, Zhi-Gang Wang, and Jian-Zhong Gu. Heavy-quark dominance and fine structure of excited heavy baryons Σ_Q , Ξ_Q' and Ω_Q . *Eur. Phys. J. C*, 84(12):1310, 2024.

[48] Hui-Zhen He, Wei Liang, Qi-Fang Lü, and Yu-Bing Dong. Strong decays of the low-lying bottom strange baryons. *Sci. China Phys. Mech. Astron.*, 64(6):261012, 2021.

[49] Kai-Lei Wang, Qi-Fang Lü, and Xian-Hui Zhong. Interpretation of the newly observed $\Sigma_b(6097)^\pm$ and $\Xi_b(6227)^-$ states as the P-wave bottom baryons. *Phys. Rev. D*, 99(1):014011, 2019.

[50] Er-Liang Cui, Hui-Min Yang, Hua-Xing Chen, and Atsushi Hosaka. Identifying the $\Xi_b(6227)$ and $\Sigma_b(6097)$ as P-wave bottom baryons of $J^P = 3/2^-$. *Phys. Rev. D*, 99(9):094021, 2019.

[51] Emmanuel Ortiz-Pacheco and Roelof Bijker. Masses and radiative decay widths of S- and P-wave singly, doubly, and triply heavy charm and bottom baryons. *Phys. Rev. D*, 108(5):054014, 2023.

[52] Yin Huang, Cheng-jian Xiao, Li-Sheng Geng, and Jun He. Strong decays of the $\Xi_b(6227)$ as a $\Sigma_b \bar{K}$ molecule. *Phys. Rev. D*, 99(1):014008, 2019.

[53] HongQiang Zhu and Yin Huang. Radiative decay of $\Xi_b(6227)$ in a hadronic molecule picture. *Chin. Phys. C*, 44(8):083101, 2020.

[54] J. Nieves, R. Pavao, and L. Tolos. Ξ_c and Ξ_b excited states within a $SU(6)_{\text{lf}} \times \text{HQSS}$ model. *Eur. Phys. J. C*, 80(1):22, 2020.

[55] Q. X. Yu, R. Pavao, V. R. Debastiani, and E. Oset. Description of the Ξ_c and Ξ_b states as molecular states. *Eur. Phys. J. C*, 79(2):167, 2019.

[56] Ahmad Jafar Arifi, Daiki Suenaga, and Atsushi Hosaka. Relativistic corrections to decays of heavy baryons in the quark model. *Phys. Rev. D*, 103(9):094003, 2021.

[57] Yi-Jie Wang, Xuan Luo, Hua-Xing Chen, Er-Liang Cui, Wei-Han Tan, and Zhi-Yong Zhou. Strong decay properties of P-wave single bottom baryons of the SU(3) flavor antitriplet 3_F . *Phys. Rev. D*, 111(7):076003, 2025.

[58] Wei-Han Tan, Hui-Min Yang, and Hua-Xing Chen. Predicted $\Xi_b(6087)^0$ and further predictions. *Eur. Phys. J. C*, 84(4):382, 2024.

[59] Qi Xin, Zhi-Gang Wang, and Fei Lu. The Λ -type P-wave bottom baryon states via the QCD sum rules*. *Chin. Phys. C*, 47(9):093106, 2023.

[60] Yasmine Sara Amhis et al. Averages of b-hadron, c-hadron, and τ -lepton properties as of 2021. *Phys. Rev. D*, 107(5):052008, 2023.

[61] Hua-Xing Chen, Wei Chen, Xiang Liu, Yan-Rui Liu, and Shi-Lin Zhu. An updated review of the new hadron states. *Rept. Prog. Phys.*, 86(2):026201, 2023.

[62] Hui-Min Yang and Hua-Xing Chen. P-wave bottom baryons of the $SU(3)$ flavor 6_F . *Phys. Rev. D*, 101(11):114013, 2020. [Erratum: *Phys. Rev. D* 102, 079901 (2020)].

[63] Guo-Liang Yu, Zhi-Gang Wang, and Xiu-Wu Wang. 1Dand 2D Ξ_b and Λ_b baryons *. *Chin. Phys. C*, 46(9):093102, 2022.

[64] Duojie Jia, Wen-Nian Liu, and Atsushi Hosaka. Regge behaviors in orbitally excited spectroscopy of charmed and bottom baryons. *Phys. Rev. D*, 101(3):034016, 2020.

[65] Hui-Min Yang, Hua-Xing Chen, Er-Liang Cui, and Qiang Mao. Identifying the $\Xi_b(6100)$ as the P-wave bottom baryon of $JP=3/2^-$. *Phys. Rev. D*, 106(3):036018, 2022.

[66] L. Micu. Decay rates of meson resonances in a quark model. *Nucl. Phys. B*, 10:521–526, 1969.

[67] R., Carlitz, M., and Kislinger. Regge amplitude arising froms $u(6)w$ vertices. *Physical Review D*, 1970.

[68] A. Le Yaouanc, L. Oliver, O. Pene, and J. C. Raynal. Naive quark pair creation model of strong interaction vertices. *Phys. Rev. D*, 8:2223–2234, 1973.

[69] A. Le Yaouanc, L. Oliver, O. Pene, and J. C. Raynal. Strong Decays of psi-prime-prime (4.028) as a Radial Excitation of Charmonium. *Phys. Lett. B*, 71:397–399, 1977.

[70] LeYaovanc. Hadron transitions in the quark model. *gordon and breach science publishers*, 1988.

[71] Yu-Bin Zhang, Li-Ye Xiao, and Xian-Hui Zhong. Possible explanations of the observed Λ_c resonances*. *Chin. Phys.*, 49(11):112001, 2025.

- [72] Pablo G. Ortega, Jorge Segovia, David R. Entem, and Francisco Fernandez. Molecular components in P-wave charmed-strange mesons. *Phys. Rev. D*, 94(7):074037, 2016.
- [73] Danielle Morel and Simon Capstick. Baryon meson loop effects on the spectrum of nonstrange baryons. 4 2002.
- [74] Pablo G. Ortega, Jorge Segovia, David R. Entem, and Francisco Fernández. Threshold effects in P-wave bottom-strange mesons. *Phys. Rev. D*, 95(3):034010, 2017.
- [75] Ru-Hui Ni, Jia-Jun Wu, and Xian-Hui Zhong. Unified unquenched quark model for heavy-light mesons with chiral dynamics. *Phys. Rev. D*, 109(11):116006, 2024.
- [76] Aneesh Manohar and Howard Georgi. Chiral Quarks and the Nonrelativistic Quark Model. *Nucl. Phys. B*, 234:189–212, 1984.
- [77] Hui-Hua Zhong, Ming-Sheng Liu, Ru-Hui Ni, Mu-Yang Chen, Xian-Hui Zhong, and Qiang Zhao. Unified study of nucleon and Δ baryon spectra and their strong decays with chiral dynamics. *Phys. Rev. D*, 110(11):116034, 2024.
- [78] Hui-Hua Zhong, Ming-Sheng Liu, Li-Ye Xiao, Kai-Lei Wang, Qi-Li, and Xian-Hui Zhong. Ω_c baryon spectrum and strong decays in a constituent quark model. 2 2025.